THE UNIVERSITY OF ADELAIDE

THE STRUCTURE OF THE MYPONGA RIVER - CARRICKALINGA CREEK AREA, SOUTHERN ADELAIDE FOLD BELT, FLEURIEU PENINSULA, SOUTH AUSTRALIA.

by DA BUHRER

November, 1995

THE STRUCTURE OF MYPONGA RIVER - CARRICKALINGA CREEK AREA, SOUTHERN ADELAIDE FOLD BELT, FLEURIEU PENINSULA, SOUTH AUSTRALIA

DANIEL ANTON BUHRER, BSc.

Thesis submitted as partial fulfilment for the Honours Degree
of Bachelor of Science

Department of Geology and Geophysics
University of Adelaide
November, 1995

National Grid Reference
(SI 54) 6527-36; 44, 45, 36, 37
1:10 000 sheets

THE MYPONGA THRUST SYSTEM

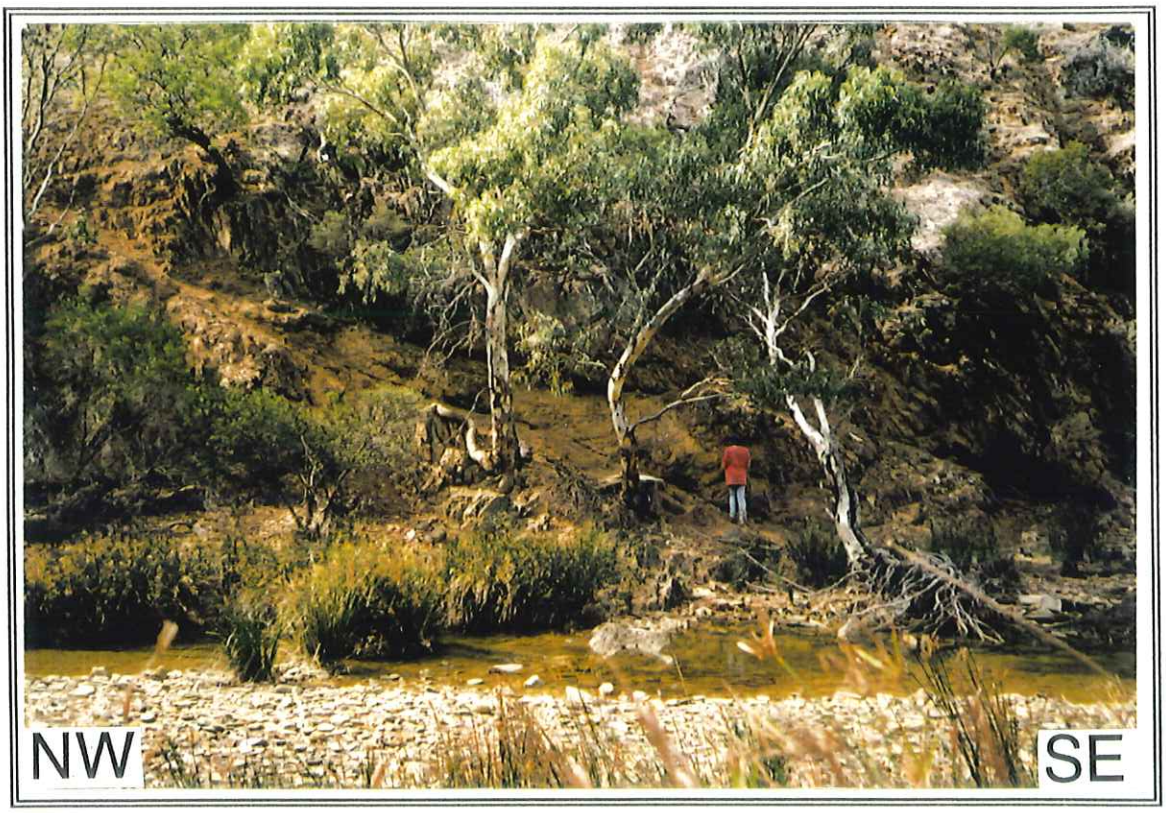

A low angle Delamerian thrust within the Myponga Duplex (Sub-Domain 3a).

CONTENTS

List of Figures

List of Colour Plates

List of Maps

ABSTRACT

The area between Myponga Beach and Carrickalinga Creek on the southern Fleurieu Peninsula was the subject of detailed geological and structural mapping. Early-middle Proterozoic Basement Complex and an overlying sedimentary prism of late Proterozoic to Cambrian age were redistributed during the Delamerian compressional event. Southeast over northwest movement induced thrusting and folding which produced a southeast hindward dipping thrust system. The deformational processes and structural geometries are similar to other classic thin skinned fold and thrust belts such as the Moine Thrust Zone in NW Scotland.

Major thrusts are generally unseen but associated with intense folding and layer parallel shear in hangingwall zones and less intense deformation in footwall zones.

Structural geometry commonly changes along strike from frontal to oblique and lateral orientations and minor folds have complex axial trace trend variations. These features are related to the morphology of the basal detachment surface which may form oblique and lateral ramps.

Individual thrusts are noted to have differential displacements along their traces (up to 4.8 km) and the spatial variation in displacement is used to reconstruct thrust sheet interactions during emplacement.

Fourteen closely spaced (50 m) imbricate thrusts define a duplex system in the more external zone. Each thrust has minor displacement and horses contain northwest vergent anticline-syncline pairs.

Major and minor folds occur throughout the study area. Minor folds mirror the larger scale structures and are generally northwest vergent steep to overturned closed folds.

A homoclinal phylitic discrete, spaced cleavage was predominant throughout the area. Its intensity increased (spacing became smaller) in proximity to major thrusts. Local crenulation cleavages and small S2 folds indicate the occurrence of a second phase of deformation.

A 45% shortening has produced high strain ratios of up to 11:1 and oblate strain ellipsoids which are recorded by elongate ooids within the Brighton Limestone.

Chapter 1

INTRODUCTION

1.1. REGIONAL SETTING AND HISTORICAL DEVELOPMENT

The Cambro-Ordovician Delamerian Orogeny (Thomson, 1969), subjected NeoProterozoic Adelaidean and early Cambrian Normanville and Kanmantoo Group sedimentary sequences to major contractional deformation and metamorphism. These rocks outcrop in a long sigmoidal shaped zone stretching from Olary in the northeast to Kangaroo Island in the southwest (Figure 1.1), which is colloquially termed the Adelaide Fold Belt (AFB). Traditionally, the AFB has been linked with the Ross Orogen of the Transantarctic Mountains in Antarctica and therefore may only be a small part of a very extensive, elongate orogenic belt similar in dimensions to the present Alpine-Himalayan chain (Manktelow, 1990).

Continuous contractional deformation of the Delamerian Orogeny produced up to three regional phases of folding (Offler and Flemming, 1968). The first and pervasive phase in the Adelaide Fold Belt south of Adelaide (SAFB) are strongly asymmetric and commonly overturned to the west. Anticlines on all scales have long, gently dipping eastern limbs and short, steeply dipping to overturned western limbs. Second and third generation structures are associated with locally developed small folds and crenulation cleavages and occur predominately in the eastern Mt Lofty Ranges. Slaty cleavage is variably developed in all fine grained rocks and commonly dips to the east.

Metamorphism related to the Delamerian Orogeny did not generally exceed greenschist facies in the majority of the AFB, although the Kanmantoo Group shows a significant metamorphic gradation across the Fleurieu Peninsula from lower greenschist facies in the west to upper amphibolite facies in the east (Offler and Fleming, 1968).

Conventionally the SAFB has been regarded as having an anticlinal structure with crystalline basement cores. Thrust faulting, although being frequently recognised (Campana and Wilson, 1955, Abele and McGowran, 1959), was given little tectonic significance. Within the last decade the Adelaide Fold Belt south of Adelaide) has been renamed and reinterpreted from the independent studies of Jenkins (1986, 1990), Steinhardt, (1991), Clarke and Powell (1989), and Flottman et al (1994), who all envisaged thrusting on a much larger scale than previously anticipated. It is now termed the Southern Adelaide Fold and Thrust Belt. Jenkins suggested that the basement inliers were allochthonous and further suggested a regional dêcollement at depth with partial basement involvement and a northwest movement. Steinhardt presented field evidence from small areas throughout the SAFB and suggested the belt now be recognised as a

fold and thrust belt. From his detailed microstructural analysis he also suggested that the deformation was much more complex than had previously been considered. He recognised six different foliations preserved in rocks from the higher grade zone.

In a broad sense, classical collisional orogenic belts in which fold thrust belts occur, can be divided into internal zones and external zones. Internal zones are characterised by ductile deformation, penetrative strains and elevated metamorphism and are also referred to as the orogenic hinterland. The external zone borders the undeformed continental interior and is characterised by less intense deformation, very low to (rarely) low grade metamorphic conditions, and non penetrative strains. The foreland of an orogenic belt refers, in a strict sense, to the undeformed region in front of the thrust belt. Sometimes, the term is used with reference to the region of diminishing shortening, comprising the most external portion of the fold and thrust belt (Marshak and Woodward, 1988). This nomenclature is adopted in ensuing descriptions and discussion.

1.2. STUDY LOCALITY AND GEOMORPHOLOGY

The study area is located approximately 60 km south of Adelaide on the western coast of the Fleurieu Peninsula, northwest of Yankalilla (Figure 1.1). It is bounded on the northern side by the Myponga Reservoir and the Myponga River. The coastline creates the western boundary while Carrickalinga Creek and the Adelaide-Yankalilla (Main South) Road form the southern and eastern boundaries, respectively. The western coastal boundary is approximately 8 km in length and the eastern boundary is located approximately 5 km inland.

The coastline curves from northeast to southwest at Myponga Beach, to north-south at Carrickalinga giving the study area a "piece of pie" shape. Limestone lithologies along the coast tend to be concomitant with the steep cliffs and rough shore platforms, which form the majority of the northern coastline. Where shales and sandstones meet the coast, south of Carrickalinga Head, sandy beaches and isolated wave cut platforms predominate.
The drainage system is oriented approximately perpendicular to the shore line with numerous bends and small branches at right angles to the main drainage direction. Creeks cut deeply into the hills forming well exposed, steep sided gullies. Drainage is also generally perpendicular to the structural grain and good cross sections can be observed in the creeks. Outcrop quality generally wanes to the south due to lower topography and less stream incision. In general the heavily grazed areas tended to procure superior outcrop. Where limestone is the dominant lithology, a karst like morphology is prevalent, with common small collapse dolines and deep caves.

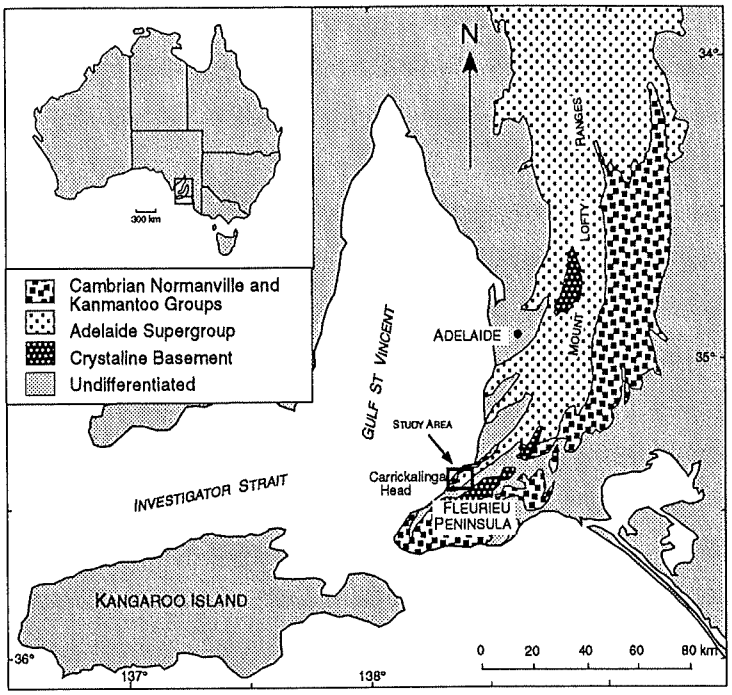

Figure 1.1. Location map of the Mt Lofty Ranges and study area. Adapted from Manktelow (1990).

1.3 PREVIOUS INVESTIGATIONS IN THE MAPPING AREA

Prior to the published study of Madigan (1925), the coast of Fleurieu Peninsula south of Sellick Hill had, to a large extent, not been visited by geologists. The results of Madigan's pioneering studies of the coastline from Sellick Hill to Victor Harbour were published as a sketch map of the geology of the Fleurieu Peninsula accompanied by several basic structural cross sections inland from Myponga Beach, Carrickalinga Head and Carrickalinga Creek. His Myponga Creek section addressed the repetition of calcareous beds which were later named Brighton Limestone. The structural significance of this repetition was not recognised at that time. Campana *et al.* (1955) produced cross sections at the same locations as Madigan and highlighted major faults and large scale folds with overturned western limbs. The first relatively detailed structural study was undertaken by Abele and McGowran (1959). Although mainly interested in the coastal Cambrian outcrops, they recognised areas and lithologies of higher strain and frontal and lateral faulting which separated Adelaidean sedimentary rocks from Cambrian sedimentary rocks. The lateral fault was recognised on the basis of structural discordancy and lithological discontinuity. The Yankalilla 1:1 000 000 map sheet produced by MESA and compiled by Preiss (1994) was generated from the South Australian Geology GIS data base and provided the most recent geological interpretation.

1.4 AIMS AND RESEARCH METHODS

The aims of this study were to:

1) produce a detailed geological and structural map of the area,
2) analyse the structural geometry including arrays of faults and folds,
3) produce balanced cross sections,
4) observe the microstructure and investigate the possible deformation mechanisms,
5) use strain analysis techniques to quantify the deformation and displacement history,
6) use all of the above to discuss the tectonic history of the mapping area and its relationship to the tectonics of the entire fold belt.

The data used to support these aims was collected from various sources. Mapping on aerial photographs at 1:10 000 scale enabled detailed documentation of foliations, lineations, fault and fold geometric properties and lithological and stratigraphic boundaries. Maps and cross sections were initially drafted by hand and later redawn using computer drafting techniques. Thin sections of field samples provided valuable evidence on microstructural relationships, including deformation mechanisms and shear sense. They also provided the raw data for strain analysis. Computer packages were utilized to gain the data sets used for strain analysis (DIGITIZE) and process the data sets into useful forms (INSTRAIN).

Chapter 2

DESCRIPTIONS OF LITHOLOGIES AND STRATIGRAPHY

2.1. INTRODUCTION

The study area comprises four stratigraphic elements: 1) an early to middle Proterozoic Basement Complex, 2) a late Proterozoic sedimentary succession comprising the Burra, Umberatana and Wilpena groups collectively known as Adelaidean, 3) an early Cambrian platformal succession, the Normanville Group and 4) an early-middle Cambrian sequence, the Kanmantoo Group (Figure 2.1). Precambrian units are rarely entirely exposed and their thicknesses are significantly increased by folding and thrusting. The outcrop limits of stratigraphic units are presented in Map 1.

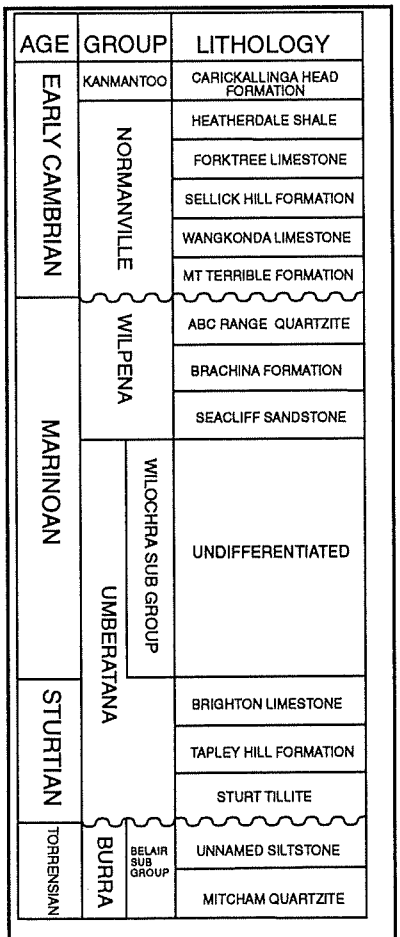

Figure 2.1. The local stratigraphy.

2.2. THE BASEMENT COMPLEX

The Basement Complex is a pale brown to grey gneiss which outcroped in the SE corner of the study area.

2.3. THE BURRA GROUP

The Belair Subgroup

Mitcham Quartzite constitutes the oldest sedimentary rocks in study area and is a highly siliceous massive to thickly bedded whitish quartzite. Its outcrop was concurrent with topographic highs and was observed only in the SE part of the study area.

2.4. THE UMBERATANA GROUP

The Sturt Tillite

Unconformably overlying the Belair Subgroup is a brown weathered, foliated conglomerate containing quartz and granite pebbles and a finer, pale, yellow and black matrix known as the Sturt Tillite (Plates 4 a and b). It outcrops as a narrow (20 m) zone in the hangingwall of a large thrust in the SE of the study area. It is generally continuous along strike, but locally pinches out against the fault (Map 2).

Segnit (1939) recorded boulders of quartzite, course grained banded gneiss, dark coloured biotite granite, fine grained to very feldspathic sandstone and vein quartz in the unit south of Myponga. The variability and abundance of crystalline basement clasts indicates a glacial derivation from complex igneous and metamorphic basement terrains composed of granodioritic gneiss, granite, adamellite, diorite and rhyolite (Preiss, 1987).

The Tapley Hill Formation

The dominant lithology of the Tapley Hill Formation is a well sorted, dark bluish-grey, slightly calcareous or dolomitic, often pyritic siltstone that commonly weathers yellow (Plate 1d). It is found extensively between the Smiths Hill Road and Carrickalinga Hill Thrusts (Map 1). The grain size and carbonate content tend to increase in the upper part of the unit.

The Brighton Limestone

The Brighton Limestone is a blue coloured, oolitic banded, siliceous limestone gradationally overlying the Tapley Hill Formation. The ooids (Plates 4d to g) have a high iron content and on weathering surfaces attain golden-yellow and redish colours. The limestone was easily recognised in the field and was found to be repeated several times. Some outcrops displayed siliceous banding rather than oolitic banding and have a serrated weathering pattern.

The Willochra Subgroup

Rocks of the Willochra Subgroup are coarse to medium grained, greenish and siliceous to feldspathic psammites or brown-grey, calcareous, dirty sandstones with pelitic interbeds. They outcrop in the NW section of Myponga River. Primary structures such as cross bedding and graded bedding can be observed in the more siliceous rocks.

2.5. WILPENA GROUP

The Seacliff Sandstone

This unit consists of medium to thick bedded, reddish and greyish feldspathic quartzite and sandstone with interbedded reddish siltstone. Outcrops were not extensive and confined to north-central areas. It is a useful marker bed that is readily recognised amongst the more pelitic units but contained little structure.

The Brachina Formation

These rocks are characteristically chocolate brown, maroon or brown and olive, drab interbedded siltstones. They outcrop extensively in the central regions of the study area and were readily recognisable. The chocolate brown siltstones are frequently interbedded with fine (1-2 cm) pale green siltstones. The contrast in colour made the tracing of bedding surfaces easy even when outcrops are weathered. The rocks are relatively ductile in comparison to the overlying and underlying sandstones and quartzites as evidenced by common folding (Plate 1a).

The ABC Range Quartzite

This unit is composed largely of pale pinkish grey, medium to coarse grained, slightly feldspathic quartzite with minor pale greenish grey, micaceous partings. It outcrops with an elongate elliptical trace in the central areas and further west is repeated several times. The quartzite is massive and readily traceable amongst the less competent underlying and overlying formations. The contact with overlying Cambrian sediments is disconformable.

2.6. THE NORMANVILLE GROUP

The Mt Terrible Formation

The unconformable base of this unit marks the Precambrian-Cambrian sequence boundary. The Mt Terrible Formation consists of cavernously weathered, calcareous, quartz rich, feldspathic sandstone and siltstone and is slightly phyllitic in the lower portions. It is similar in colour to the ABC Range Quartzite but is distinguishable by its fissile nature and finer texture. Several repetitions were evidenced in the west central study area, but outcrops are otherwise infrequent.

Wangkonda Formation

Small outcrops of this yellow calcareous sandstone, siltstone and mottled limestone are confined to the centre of the study area. Map 2 shows the location of two oval shaped outcrops of the Wangkonda Limestone and another occurrence further to the west.

Sellick Hill Formation

This unit consists of interlayered blue to grey limestone and sandy buff to brown calcareous siltstone. The difference in layer composition is exaggerated by weathering and a serrated pattern is characteristic. It outcrops along the coast southwest of Myponga Beach and further to the south and inland. Fresh outcrop is observed in the Carrickalinga Council Quarry.

The Forktree Limestone

This Cambrian limestone is the most extensively outcropping unit. It can be subdivided into two separate units. The lower is a massive bluish grey Archaeocyathal limestone that is much thicker than the upper massive mottled limestone and siltstone, which has a serrated weathering pattern. They generally outcrop towards the coast. Bedding surfaces in both units were difficult to detect.

The Heatherdale Shale

This unit is a yellow, pink and maroon coloured shale which outcropped in the west of the study area, close to the coast. Nodules of phosphate, which are elongate and parallel to bedding planes, are common. This unit is usually heavily weathered or buried by soil. Large (30-40 cm) ellipsoidal concretions are characteristic of shale outcrops.

2.7. THE KANMANTOO GROUP

The Carrickalinga Head Formation

The Carrickalinga Head Formation, the basal unit of the Kanmantoo Group, rests conformably on the Heatherdale Shale or is faulted against Adelaidean sediments. It is comprised of three members. The lower, Madigan Inlet Member, has only 80 metres of exposure at Carrickalinga Head and consists of alternating green impure sandstone and thin olive coloured shales.

Chapter 3

STRUCTURAL GEOMETRY

3.1. INTRODUCTION

The Delamerian contractional event resulted in south-east over north-west directed displacement. Within the study area, a brittle-ductile thrust system with foreland verging thrusts (NW) and bedding and cleavage foliations that generally dip towards the hinterland (SE) are developed.

Three major SE dipping thrusts can be traced across the study area (Figure 3.1), namely from SE to NW, the Smith's Hill Road Thrust (SHRT), Carrickalinga Hill Thrust (CHT), and Black Hill Thrust (BHT). All of these trend in a broad curve from NNE in the SW to ENE in the NE, where they also become more spaced. The number of thrusts changes along strike due to a lateral connecting structure, the Derinda Dawn Fault (DDF). DDF has a branch point on the BHT and also terminates a thrust striking perpendicular to the movement direction (frontal thrust), the Goldsmith Thrust (GT). An oblique connecting thrust, the Stacey Thrust (ST), has branch points on CHT and BHT and separates a zone of folding in the SW from a zone of imbricate faulting to the NE.

Thrust surfaces were not necessarily everywhere visible in outcrop but can be mapped using structural discordance and lithological discontinuities. A zone of increased folding intensity, shearing and the general strain state of the rocks was associated with thrust surfaces. The width of this zone depends on the rheology of hangingwall and footwall rocks. Thrust surfaces appear to be moderately inclined to the SE and linked at depth by a sole thrust and form a thrust system, the Myponga Thrust System. The thrust system is generally forward breaking and in sequence. Reverse sense kinematic indicators were observed for some thrusts (Chapter 4) and a reverse nature was suggested for all thrusts from juxtaposition of younger footwall stratigraphy with older stratigraphy of the hangingwall rocks. The Normanville Thrust (NT) has a crystalline basement hangingwall which suggests a deeper thrust structure. This study did not extend to the NT and its position is taken from the MESA Yankalilla 1:1000 000 map sheet (Preiss, 1994).

Major folds were observed in all thrust sheets and minor folds were observed in the majority of the study area. Minor folding features were found to be associated with major fold features. The majority of folding is tight to closed, steep to overturned and NW vergent, but becomes increasingly open to the NW (Plates 1c to f). Fold orientations were complex (see Map 4). Distinct areas within thrust sheets (zones) exhibit fold axial traces that parallel major

thrust strike and are perpendicular to the movement direction but become oblique to laterally oriented in other zones. Fold plunge was generally gentle. Movement direction was assumed to be perpendicular to the major fault strike and major fold traces.

The intersection of bedding surfaces and cleavage (intersection lineation) is parallel or approximately parallel to minor fold axes and were grouped and analysed together with minor fold axial trace orientations.

Cleavage foliations are mostly homoclinal and steeply SE dipping with a few steep westerly dipping exceptions. Cleavage in outcrop became more closely spaced approaching large thrusts and associated shear zones and was more apparent in the pelitic than psammitic lithologies. Total grain reorientation to the extent of overprinting of all bedding traces was noted in some zones. In these cases bedding was recognisable only in the hinges of folds where bedding and cleavage were at high angles.

For further detailed discussion the study area was divided into 6 domains and sub domains (Figure 3.1) each of which contain essentially homogeneous structural geometry and structural styles related to the intensity of deformation. These domains are divided by the major thrusts. Where there is sufficient structural data, stereographic analysis has been segmented into these separate domains to highlight any variances in structural geometry (Maps 2, 3 and 4).

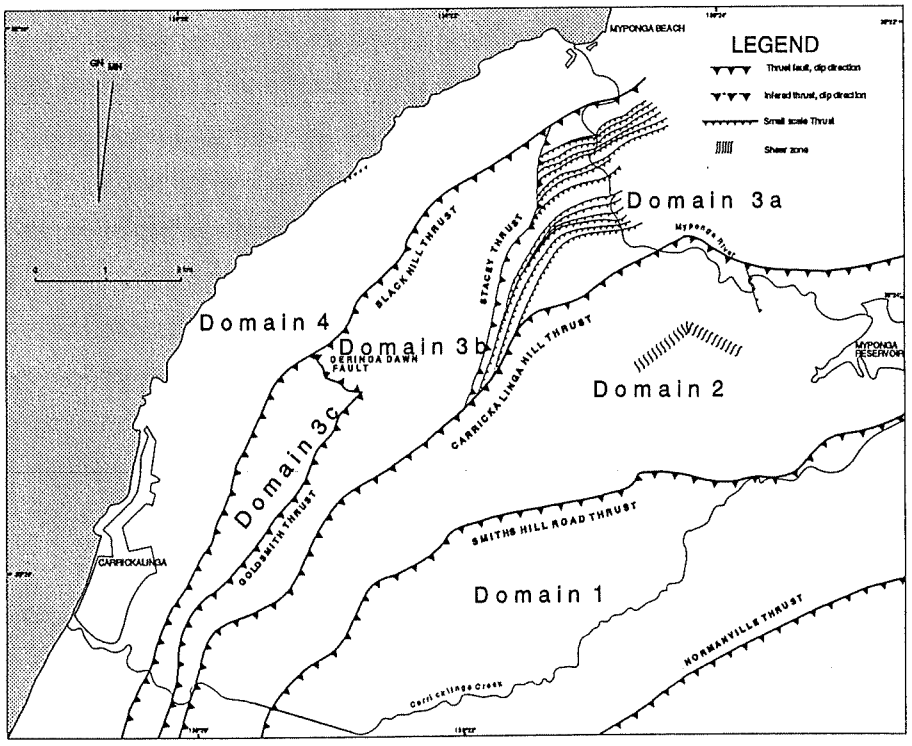

Figure 3.1. Major structure nomenclature and structural domains.

3.2. DOMAIN 1: THE SMITH'S HILL ROAD THRUST SHEET (SHRTS)

The dominant structural element within Domain 1 is a major NW verging overturned anticlinorium with a fold axial trace that generally trends parallel to the SHRT. Belair Subgroup outcrops are observed to pinch out against the SHRT and reappear further to the NE (Map 1). This outcrop shape is believed to be associated with the double plunging geometry of the major anticlinal structure. Overturning is suggested by outcrop of Sturt Tillite in the hangingwall of the SHRT which dips moderately SE and is found to underlie older Belair Subgroup rocks. Meso scale (10 m) folds which show a closed, overturned to asymmetric nature can be observed 200 m north of a Quarry adjacent to Wattle Flat Road. They are parasitic to the major fold structure and mirror its style.

3.3. DOMAIN 2: THE CARRICKALINGA HILL THRUST SHEET (CHTS).

Similar to Domain 1, the dominant structural feature of Domain 2 is a major overturned anticline. It has an axial planar trace parallel to the CHT and is doubly plunging. A Brighton Limestone marker bed within the limb closest to the foreland (forelimb), is parallel to the CHT, dips SE in the direction of the hinterland (hindward) and is underlain by older Tapley Hill Formation. Sedimentary facing directions, from outcrop within the forelimb zone reinforce an overturned nature. A stereoplot of Domain 2 bedding readings (Map 2) shows steep dips in the overturned forelimb and shallower dips, in the hindlimb, indicative of an overturned structure.

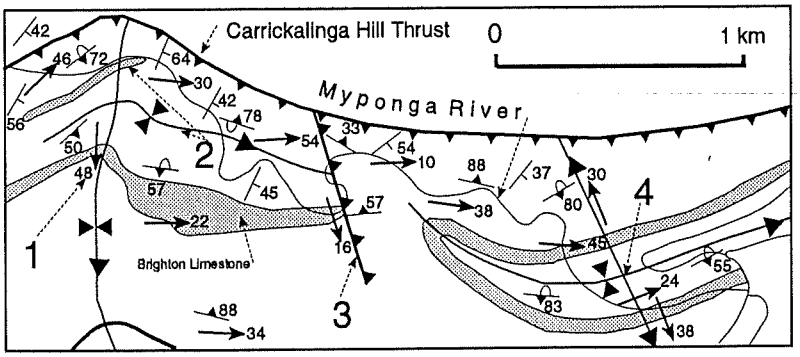

Figure 3.2. Inset of Map 1. The oblique geometry in the northeast of Domain 2.

The north east part of Domain 2 has a fold and fault geometry that is oblique to the movement direction (Figure 3.2). Stereoplots of bedding and minor fold orientations (Map 2 and 3 consecutively) show that in this region bedding and minor fold axial traces strike approximately east to west in comparison to the southwest to northeast orientation of the remainder of the thrust sheet. Cleavages in this oblique zone are persistent in orientation to those throughout the study area and folds plunge gently to the east. A kink in the Brighton

Limestone marks the transition from frontal to oblique orientations (1; Figure 3.2). In this zone minor fold axial traces strike oblique to movement directions and plunge anomalously steep to the SSE. In the oblique zone the Brighton Limestone marker bed outlines a complex geometry. Repetition of the limestone suggests a 500 m overturned syncline (2; Figure 3.2) and discontinuity of the limestone to the east suggests a fault structure (3; Figure 3.2). In its vicinity large quartz vein arrays, complex local minor fold orientations and uncharacteristic river morphology all add to the evidence for a fault oriented obliquely to the structural grain and transport direction. Further to the east minor fold axial traces strike parallel to this oblique fault and are doubly plunging. The Brighton Limestone outcrop in this area is crescent shaped and closes westward suggesting fold interference patterns of two perpendicular folds (4; Figure 3.2). Two rock samples from within the oblique zone (see appendix 1 for precise location) show exceptional evidence of both compressional and strike slip stresses (transpression) (Plate 3 a to c). These rocks show minor folds in psammite which have axial traces that plunge gently to the east indicating local N-S compression. The fold exhibits tension gashes indicative of E-W brittle dextral shear and together indicate dextral transpression. An oblique compressive stress would account for both of these features.

Folding on a 10 m scale is prevalent throughout the domain and is parasitic to the major anticlinal structure. Minor folds throughout the study area were classified after Ramsay (1967). Appendix 2 outlines and applies the classification methods used. Minor folding, recognised mainly from hangingwall and footwall zones of the thrust sheet, all show foreland vergent, asymmetric, gently plunging fold features (for precise locations see appendix 1). Minor folds in footwall rocks show close to moderately open 1c and 3, and rare 2, 1a and 1b folds. Hangingwall rocks show close 3, 1c and rare 2 folds.

Two examples of crenulation cleavage were observed from NE parts of the domain and are possible evidence for a second deformation. This is further discussed in chapter 7.

A zone of high shear is observed in the central-northeast part of the thrust sheet and seems to coincide with the major scale anticlinal axis. The shear zone fabric is described in chapter 5.

3.4. DOMAIN 3

Domain 3 is defined to contain all rocks between the CHT and BHT. It has been divided into three sub domains which show different styles of shortening.

3.4.1. Sub Domain 3A: The Myponga Beach Duplex

Sub Domain 3a is separated from Sub Domain 3b by an oblique-lateral link thrust which has branch points on CHT and BHT. It is structurally dominated by small scale, closely spaced, mostly parallel, imbricate type thrusting which overprints an original major syncline. Rocks of the Brachina Formation outcrop in a SW closing outlier in the central southeastern half of Sub Domain 3a and form the core of the major syncline (Map 1). Steep NW dipping and overturned SE dipping Seacliff Sandstone and rocks of the Willochra Subgroup form the hindlimb. Forelimb rocks, from the core of the syncline to the BHT, outcrop sequentially as Seacliff Sandstone, rocks of the Willochra Subgroup, Brighton Limestone and rocks of the Tapley Hill Formation. Facing of primary structures, including cross bedding and graded bedding within sandier units of the Willochra Formation, provide evidence in support of an overturned hindlimb.

The first evidence for small scale imbricate thrusting is multiple repetition of the Brighton Limestone. Three repetitions within 200 m were observed on a traverse up the first tributary of Myponga River. Along strike, in the Myponga River, two closely spaced high angle faults are observed in profile in the valley wall. The breaks are discrete and defined by a 5-10 cm zone of highly strained, fine grained, pale pelite. This is the style of faulting throughout Sub Domain 3a (Plates 1a and b) and 14 imbricate thrusts were recognised and believed to form a link thrust duplex system. The number of imbricate thrusts changes along strike due to branching and diverging to the NE. Displacement on each imbricate thrust is small (< 100m). True lithological boundaries are rare and more often transpire due to juxtaposition upon imbricate thrust surfaces.

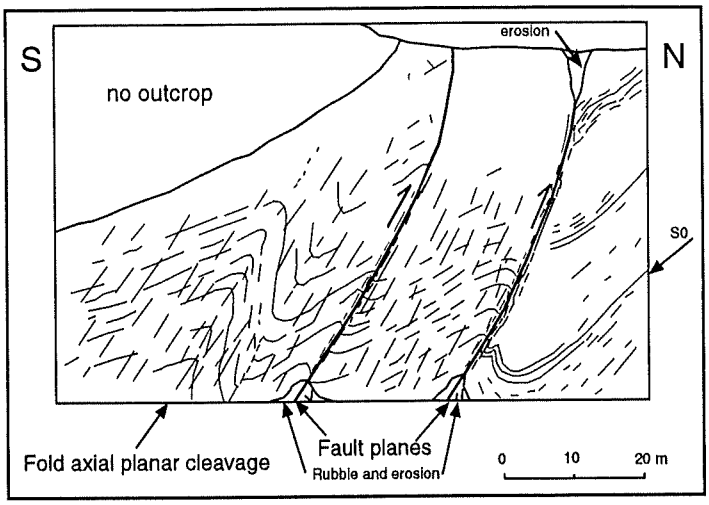

Figure 3.3. Imbricate thrusts from Sub Domain 3a.

Plate 1a and figure 3.3 show two homoclinal link thrusts in outcrop from Myponga River. The rocks between the link thrusts (horse) have a footwall syncline and hangingwall anticline. This folding pattern was generally repetitious within each horse as is depicted in the admissible state cross section through the Myponga Beach Duplex (Figure 3.4). The duplex classification of Mitra, (1986), places the Myponga Duplex into a class 1B hinterland sloping category, where the majority of thrusts have a small spacing and relatively small displacements. The roof thrust slopes shallowly toward the hinterland while the imbricate thrusts dip more steeply in same direction and anticline syncline pairs are developed within horses (Figure 3.4).

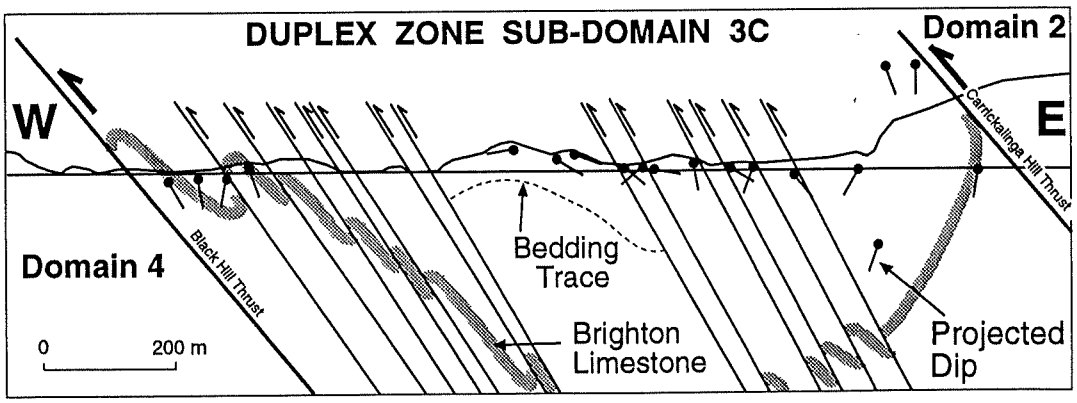

Figure 3.4 An admissible state cross-section through the Myponga Duplex. Projected bedding constrains an anticline-syncline nature within each horse. The Brighton Limestone marker bed is repeated in surface outcrops of foremost regions by duplex thrusting. The broad syncline is a major feature of the sub domain and is constrained by bedding data. Note the small offsets across each duplex thrust. The Brighton Limestone bedding trace is not shown in the centre of the figure since it forms a synclinal core.

The sub domain is bordered to the SW by ST which has a northern lateral component and a southern oblique component. Imbricate link thrusts are truncated by the lateral portion of Stacey Thrust and are parallel to the oblique portion. The latter are truncated by the CHT.

Stereographic analysis of bedding (Map 2) shows a general NE strike with dips mostly SE, but varies to shallow SW, shallow NW and steep NW. These readings would be expected with anticline-syncline folds. Analysis of minor fold orientation (Map 4) reveals two dominant shallow plunge directions which are complex in their spatial distribution. Minor folds in the sub domain were classified (Appendix 2) as NW verging, close, tight-angular, buckle-mushroom 1c folds (Plate 1e and f).

3.4.2. Sub Domain 3B

Sub Domain 3b is bound by CHT, ST, BHT, DDF and GT. The rocks are dominated by folds of different wavelength, amplitude and orientation. In the south, a major NW vergent, overturned, doubly plunging syncline has two oval shaped Cambrian Wangkonda Limestone outliers as cores. Surrounding these is a closed outcrop of ABC Range Quartzite. The northern end of this syncline is more complexly folded and is discontinuous. To the east three repetitions of ABC quartzite and Mt Terrible Formation suggest multiple open NW vergent folds which plunge gently south. Directly adjacent to DDF they are oriented parallel to BHT, but further north curve towards and become oblique to the BHT (Map 1). These lithologies are discontinuous to the north where rocks have a complex geometry. To the west of ST a pale green shale, assumed to be a lower part of the Brachina Formation due to similarities in colour and texture of the green banded units, is traced as an elongate sigmoidal outcrop parallel to the ST. Bedding dips approximately 50° to the west and is believed to be associated with the forelimb of an open, NW vergent anticline. Stereographic analysis of bedding readings (Map 2) show a strong differentiation between steep SE and steep NW dips as would be expected from angular non overturned folds. Similar analysis of minor fold orientations (Map 4) shows a dominant south directed gentle plunge and a scatter of north through east to south plunge directions. A zone east from the point of contact of GT and DDF shows anomalous geometry. Minor fold orientations are steep (67°) SE plunging and the ABC Range quartzite is deflected into a Z shape and believed to be a fold interference feature. The Wangkonda Limestone core has been bisected into two oval outliers. This is due to fold interference. Minor fold analysis throughout the sub domain indicates tight, angular, NW verging and rarely overturned, 1c and 3 folds.

3.4.3 Sub Domain 3C

This sub domain is dominated by major open folding. An oval shaped outlier of Forktree Limestone in the NE forms the core of a shallow SW plunging syncline structure with a steep NW to vertical hindlimb. The hinge has a Z trace and is truncated by the BHT. Bedding adjacent to DDF parallels the fault and strikes SE. Outcrops of Wangkonda Limestone and Mt Terrible Formation west of the Forktree outlier have a cuspate shape and are truncated by the BHT. Based on field observations, a second SE plunging syncline structure exists and creates a dome/basin pattern fold geometry by superposition of two perpendicular folds. To the south bedding is near vertical or dips steeply west. Stereographic analysis shows an average strike of N16°. The Carrickalinga Council Quarry is central to the thrust sheet and provides fresh outcrop of Sellick Hill Limestone.

3.5 DOMAIN 4

Domain 4 is dominated by broad, open, asymmetric, major folds which plunge gently south. Minor fold orientations provide evidence for plunge reversal in the NW footwall of BHT. Stereographic analysis shows an average strike of N38° with 50-60° dips. A thrust feature with a steep surface (60°) is observed in coastal outcrop near to the SHL-Forktree lithological boundary. It has sub-horizontal, undeformed footwall rocks and steep NW dipping hangingwall rocks with 20 cm syncline anticline pair directly adjacent to the thrust surface.

MAP 1: MYPONGA RIVER - CARRICKALINGA CREEK GEOLOGY

LITHOLOGY

- Kanmantoo Group-
  - Carrickalinga Head Formation
- Normanville Group
  - Heatherdale Shale
  - Forktree Limestone Unit 2
  - Forktree Limestone Unit 1
  - Sellick Hill Limestone
  - Wangkonda Limestone
  - Mt Terrible Formation
- Wilpena Group
  - ABC Quartzite
  - Brachina Formation
  - Seacliff Sandstone
- Umberatana Group
  - Undifferentiated Willochra Fm.
  - Brighton Limestone
  - Tapley Hill Formation
  - Sturt Tillite
- Burra Group-
  - Belair Subgroup
- Basement-Complex

LEGEND

- Bedding, dip, strike, overturned bedding
- Cleavage foliations, dip, strike
- Intersection lineations, minor fold axes, plunge, plunge direction
- Fold axial trace, anticline, overturned anticline, plunge direction
- Fold axial trace, syncline, overturned syncline, plunge direction
- Thrust fault, dip direction
- Imbricate thrust
- Lithological boundaries
- Shear zone
- Roads
- Elongation lineation
- Rivers, creeks
- Vein fibre lineations
- Quarry

0 1 2 km

Inset for Figure 3.2

Myponga River

MYPONGA BEACH

MYPONGA RESERVOIR

CARRICKALINGA

Smiths Hill Road

Wattle Flat Road

Carrickalinga Creek

Adelaide - Yankalilla Road

NORMANVILLE THRUST

A

A'

B

B'

GN MN

138°20'

138°22'

138°24'

35°22'

35°24'

35°26'

LOCALITY MAP

- Cambrian Normanville and Kanmantoo Groups
- Adelaide Supergroup
- Crystaline Basement
- Undifferentiated

ADELAIDE

GULF ST VINCENT

INVESTIGATOR STRAIT

KANGAROO ISLAND

FLEURIEU PENINSULA

Carrickalinga Head

STUDY AREA

MOUNT LOFTY RANGES

0 20 40 60 80 km

MAP 2: MYPONGA RIVER - CARRICKALINGA CREEK BEDDING READINGS

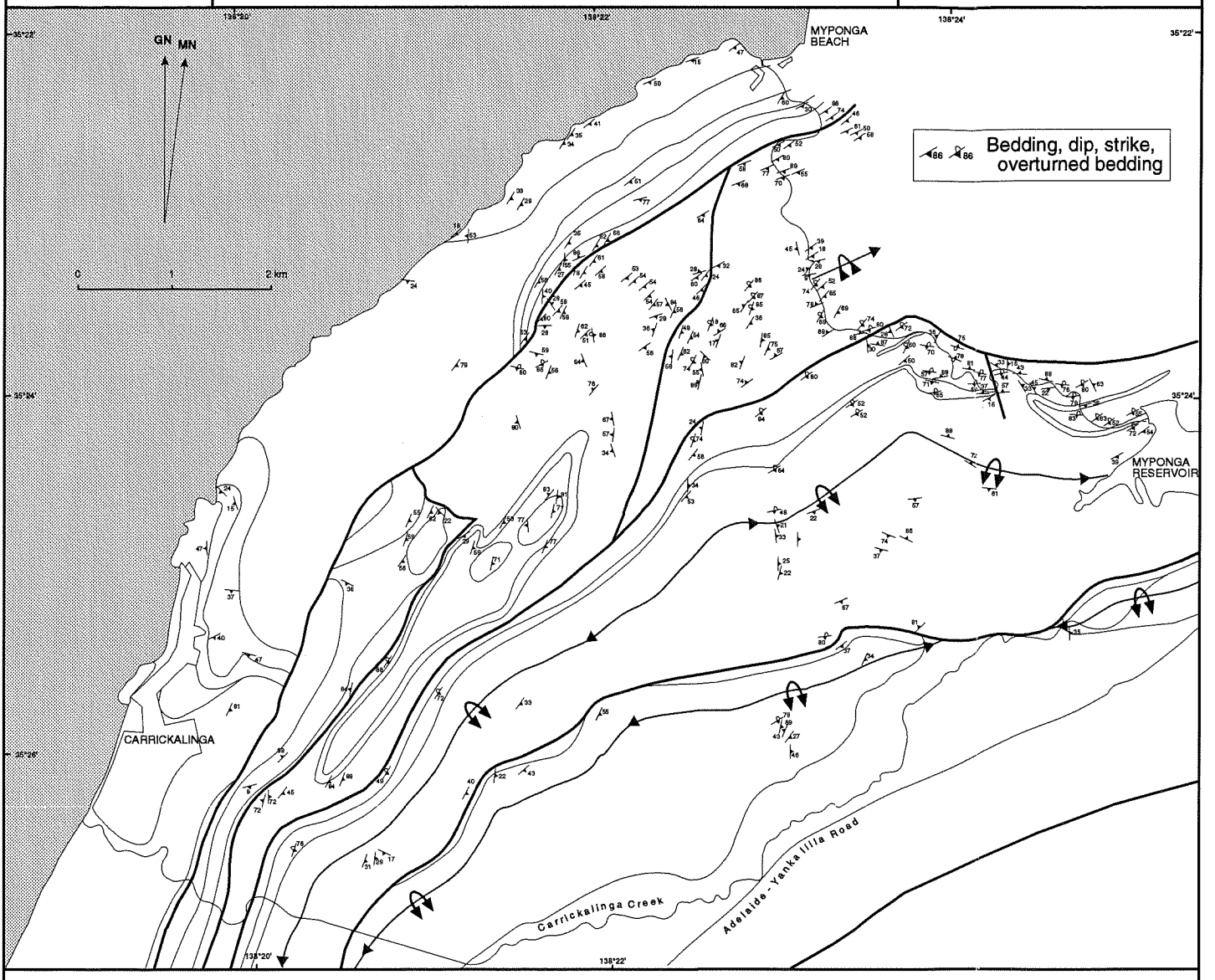

DOMAIN 1

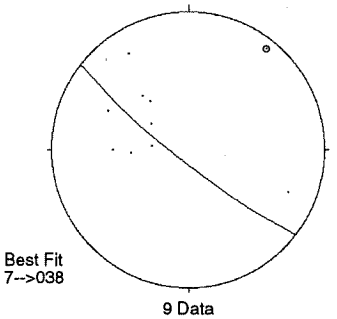

Best Fit
7-->038

9 Data

DOMAIN 2

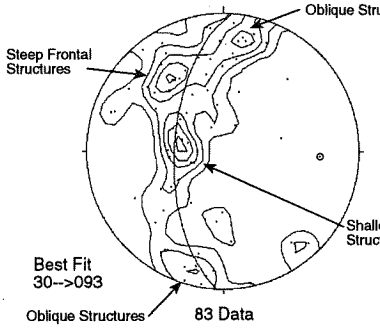

Best Fit
30-->093

83 Data

SUB DOMAIN 3a

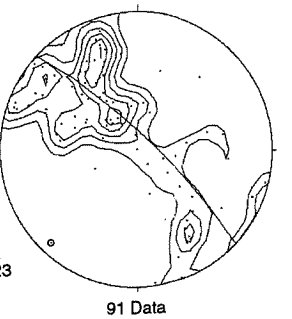

Best Fit
08-->223

91 Data

SUB DOMAIN 3b

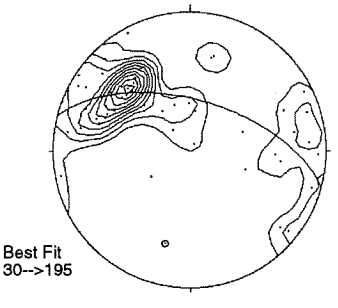

Best Fit
30-->195

56 Data

SUB DOMAIN 3c

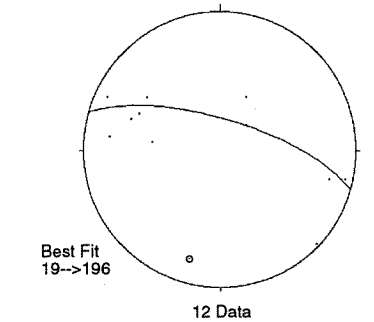

Best Fit
19-->196

12 Data

DOMAIN 4

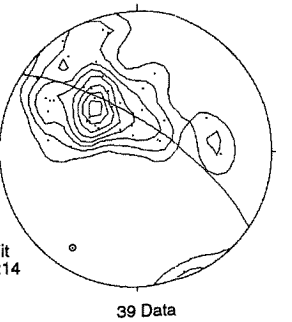

Best Fit
16-->214

39 Data

MAP 3: MYPONGA RIVER - CARRICKALINGA CREEK | CLEAVAGE READINGS

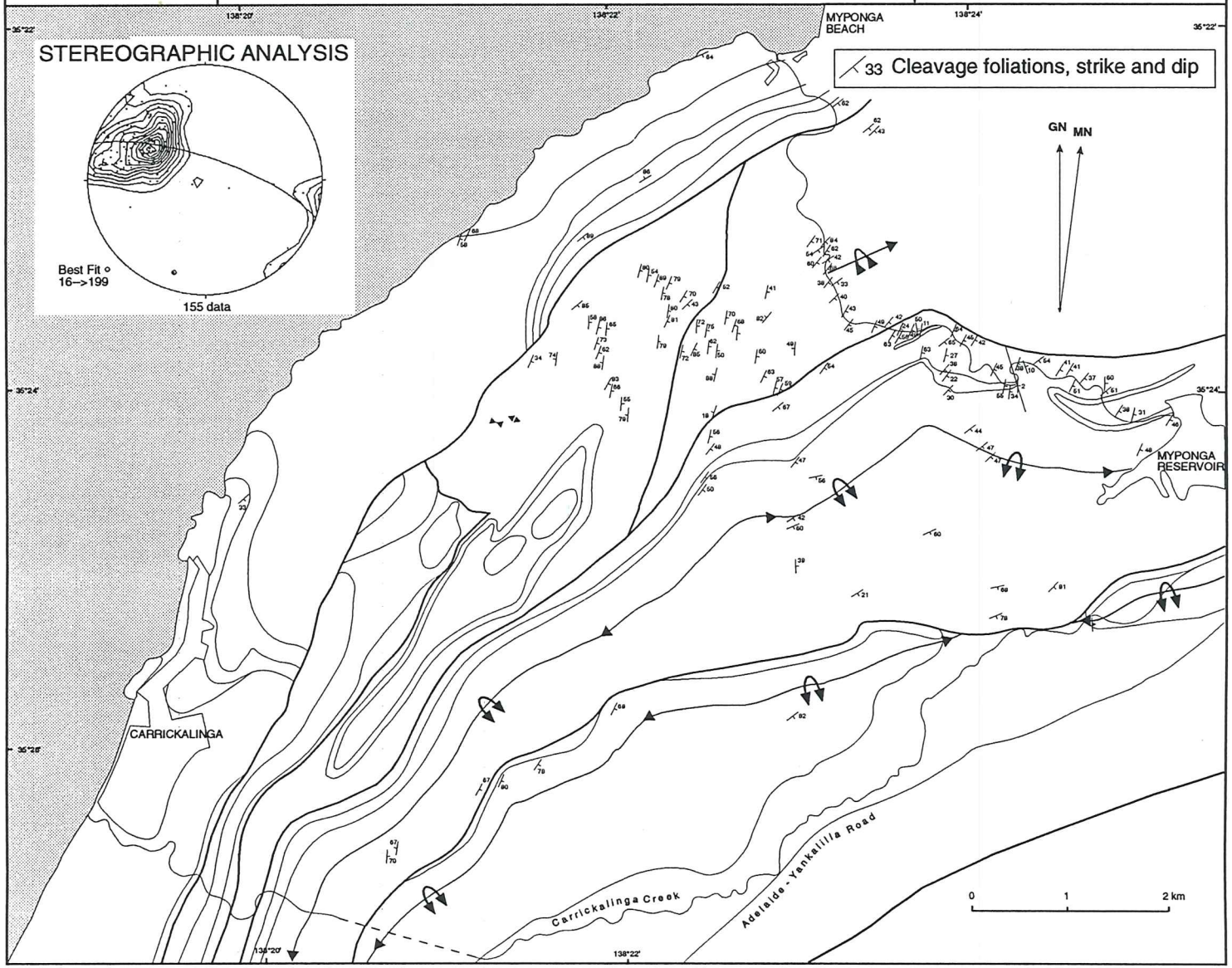

MAP 4: MYPONGA RIVER - CARRICKALINGA CREEK

Minor fold axial trace orientations and intersection lineations

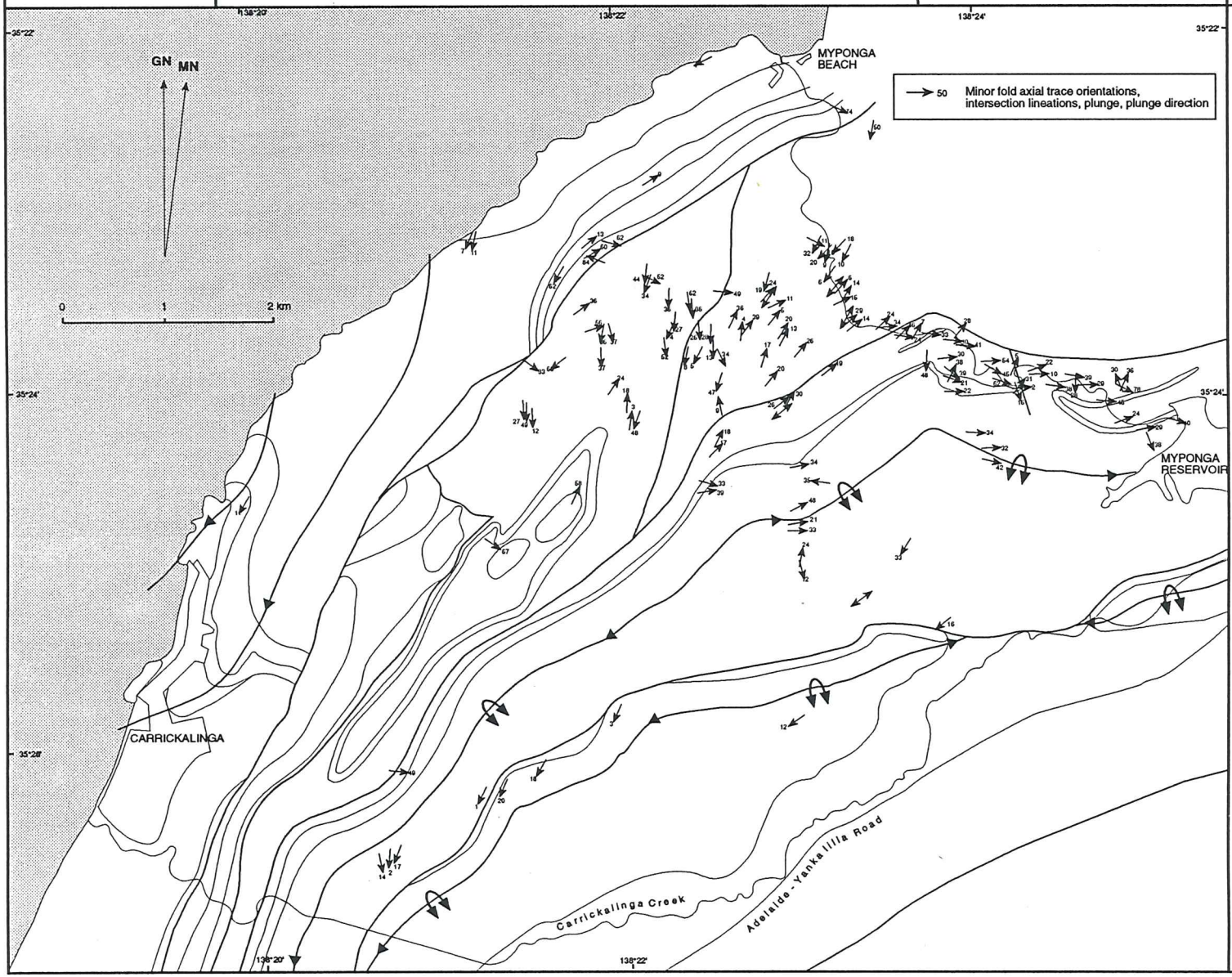

STEREOGRAPHIC ANALYSIS

DOMAIN 2

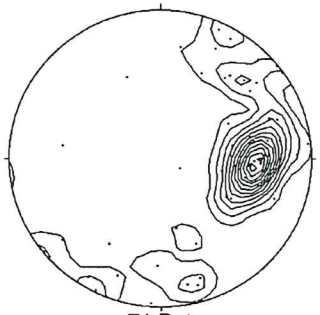

71 Data

SUB DOMAIN 3a

56 Data

SUB DOMAIN 3b

26 Data

PLATE 1 DESCRIPTIONS

Plate 1a. Two NW vergent imbricate faults and associated folding in Sub Domain 3a. Note the anticline syncline pair in the horse and the hangingwall of the SE most thrust. Field of view, 60 m. Location 37-3-36.

Plate 1b. A NW vergent imbricate thrust from Sub Domain 3a. Field of view, 10 m.

Plate 1c. A NW verging overturned anticline. Location 37-4-73.

Plate 1d. Intense folding in the Tapley Hill Formation. Location 155-1-23

Plate 1e. A small, tight, overturned anticline. Location 155-1-18.

Plate 1f. A buckle fold in the Willochra Sub Group. Location 37-4-10.

PLATE 1

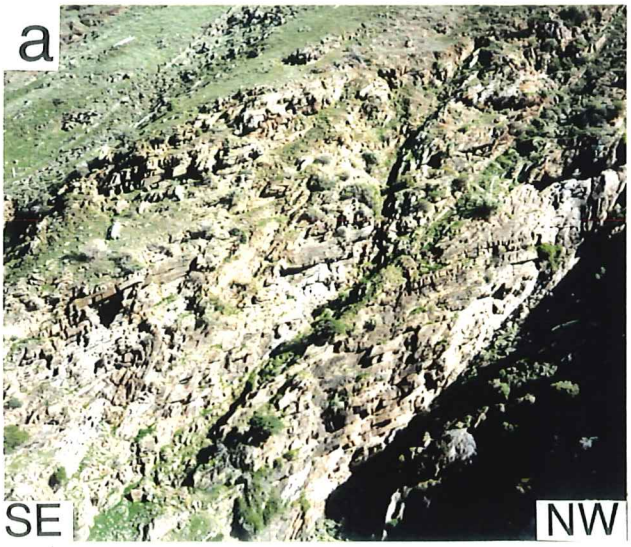

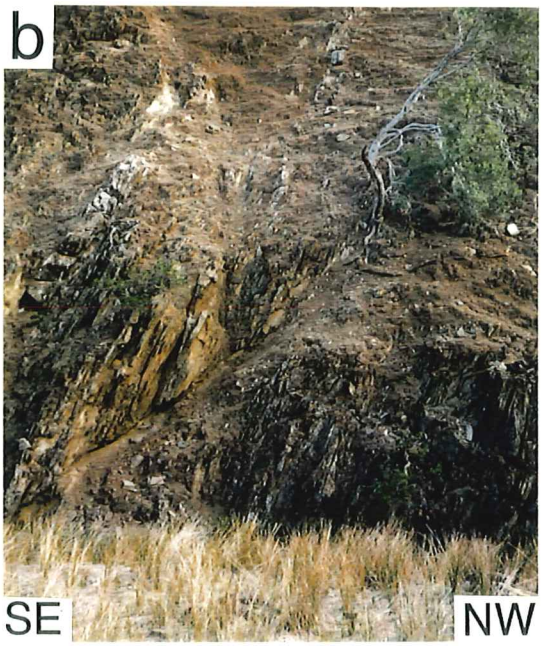

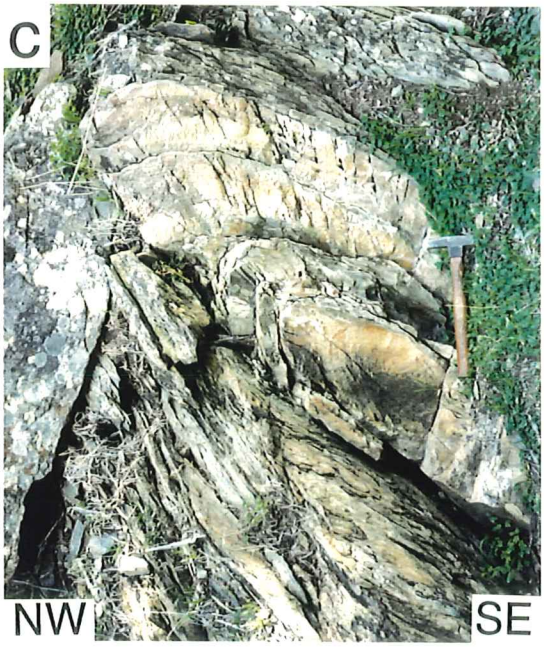

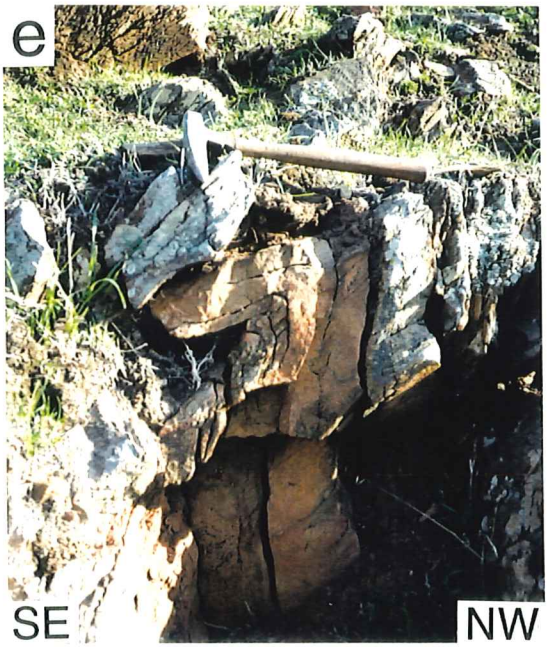

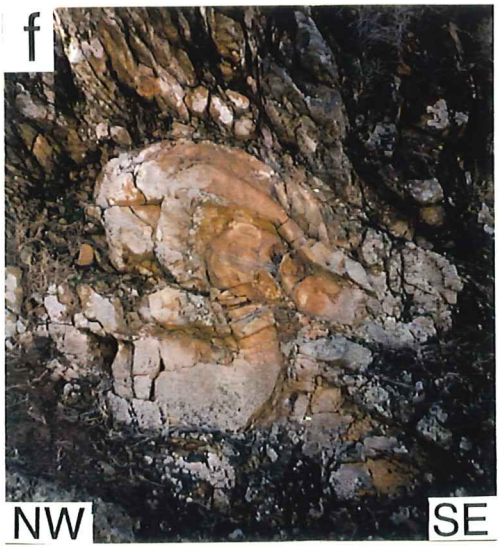

PLATE 2 DESCRIPTIONS

Plate 2a. Evidence for transpression from the oblique zone in the NE of Domain 2. The specimen is folded and has a horizontal axis in this photo. Note the evenly spaced tension gashes. Location 37-1-69.

Plate 2b. A profile view of the fold.

Plate 2c. A plan view of the fold shows en echelon and slightly sigmoidal tension gashes which in this plate indicate sinistral movement. The fold axis horizontal.

PLATE 2

a

b

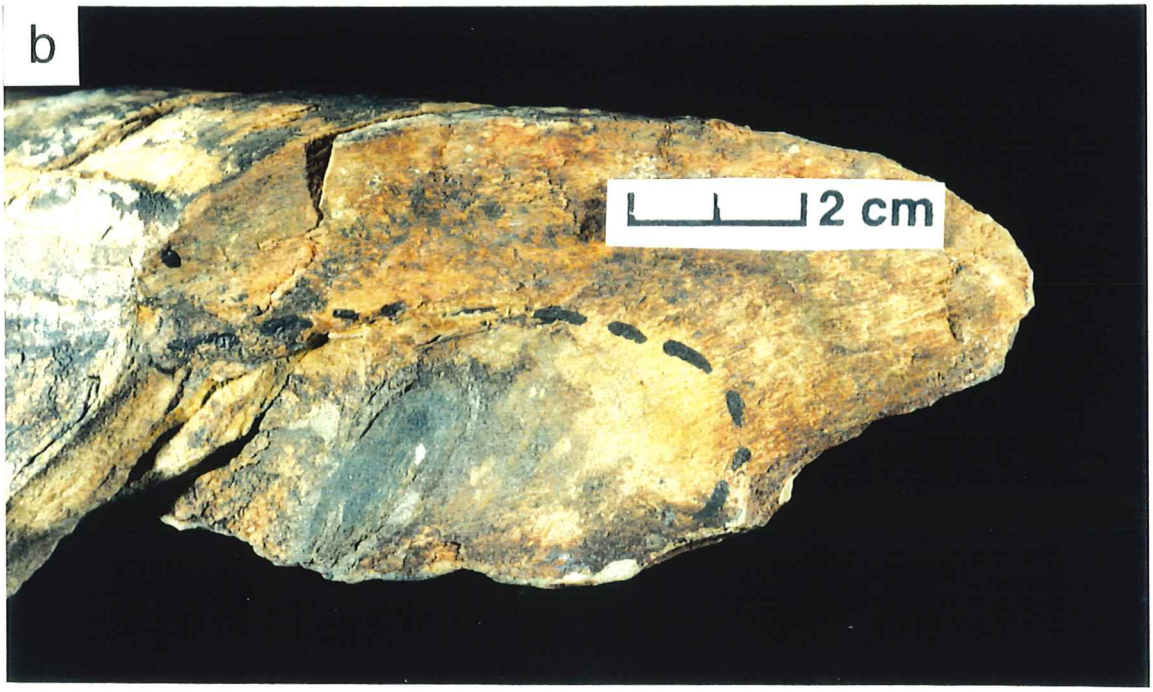

c

Chapter 4

CROSS SECTIONS

4.1. INTRODUCTION

Cross sections are very important tools for communicating information about geologic structures, so the interpretation depicted on a cross section must be as close to the truth as possible. The procedure of *cross section balancing* has become popular in recent years as a means of helping to analyse and improve cross sections. Cross section balancing permits geologists to test the validity of the structural geometry portrayed on a cross section. It requires thoughtful analysis of fault shapes, bed lengths, and cross-sectional areas. One of the key steps involved in the procedure is *restoration* of the beds depicted on the cross section to the relative positions that they had prior to deformation (Marshak and Woodward, 1988).

4.2. CROSS SECTION CONSTRUCTION AND BALANCING

The construction and balancing of the cross sections was undertaken by methods outlined in Marshak and Woodward (1988). To begin, some assumptions had to be made. A stratigraphic template was needed which represented the thickness of all observed and predicted lithologies in the area. Thicknesses from previous workers are overestimated in most cases due to the structural complexity of the rocks. Measurements of thicknesses were calculated directly from the field map or previous mapping, taking into account any folding and thrusting. The orientations of the section lines attempted to parallel the transport direction of the thrusts which was assumed to be perpendicular to the major frontal thrust strike and major frontal fold hinges. Assuming cylindrical folding and uniform local fold plunge, bedding data was projected from a maximum of 800 metres either side of the section line and corrected to true dip values by calculating the intersection lineation between the cross section plane and bedding plane. Because major thrust surfaces were not generally observable in outcrop their surface inclinations were assumed to be sub parallel to cleavage, a feature of the observable link thrusts in Sub Domain 3a, and drawn with 50-60^{o} SE dip. Sections were constructed from lithological boundary data and dip constraints using an assumption of constant bed thickness. Where bedding was poorly constrained major scale folds were constructed to mirror local minor scale folds, a relationship which was generally validated by outcrop. The construction assumes plane strain deformation geometry which requires that rocks have not moved into or out of the plane of cross section. This also involves an area conservation assumption whereby no rock volume is lost during deformation (Marshak and Woodward, 1988). This assumption was not always established due to volume loss (maximum of 15.8 %, described in chapter 5) associated with spaced cleavage and pressure solution shortening near major thrusts.

Cross section reconstructions were carried out using bed length balance which assumed that during deformation the length of a lithological contact is the same in both deformed state and restored state cross sections

4.3. THE MYPONGA THRUST SYSTEM

A thrust system is an array of kinematically related faults that develop in sequence during a single regional deformation and are associated with deformation above a basal detachment (Marshak and Woodward, 1988). The balanced, deformed state cross sections through the study area (Figure 4.1a and b) show several thrust sheets stacked upon one another and indicate that all major thrusts are primarily or secondarily linked to a deep sub-horizontal dêcollement. The study area can now be termed the Myponga Thrust System.

The recognition of fault bend fold geometry has become a basic tool for the construction of balanced cross sections and for determining the structure of thrusts at depth (Suppe *et al.*, 1992). Broad open folding within domain 4 was interpreted as being associated with a frontal ramp-flat geometry at depth where hanging wall rocks moving over a step like fault are folded or bent to accommodate the changes in fault shape. In the construction procedure the geometry of the ramp flat structures were governed by surface dip constraints. The depth to detachment of structure was more flexible with numerous acceptable possibilities considered. In both cross sections the frontal thrusts are shown to continue to the surface. This was invoked for completeness of cross section construction. Studies by Szmidel (1995) and Preiss (1994) suggest that a frontal thrust does exist and is evident north of Myponga Beach, but trends SW and is located off-shore. Cross sections AA' and BB' have ramp structures which are 1 km and 1.2 km high, respectively, and strike generally perpendicular to the transport direction, although very probably become oblique along strike as suggested by the axial trace deviation of the major folds. The frontal ramp fault structures crosscut the stratigraphy down to the sediment-crystalline basement interface where the sub-horizontal dêcollement is believed to reside. Along the CHT the basal dêcollement cuts down sequence again. Towards the more internal zones (SE) the hanging walls of the CHT, SHRT and NT contain basement and a deeper detachment is suggested. The Normanville Thrust carries basement to the surface and has a minimum average displacement of 5.4 km. This major thrust is a root thrust and dives deeper into the basement, presumably to crustal depths of 10 to 20 km. These features give the basal detachment a SE step down nature. Its level in the crust would invariably be dependant on the detailed rheology and pre-existing weakness present in the rocks.

Thrust displacement was measured as the arc length between cut off points in the hangingwall and footwall of a particular thrust. All thrusts show reverse displacement with movement on individual thrusts varying from 50 to 4800m from near surface calculations (individual displacements are displayed in figures 4.1a and b). The distance between cut-offs for different units offset along the same fault is observed to be variable on most thrusts. This feature can be explained by the occurrence of simple shear along bedding planes in the thrust sheet or the partitioning of strain between fault displacement and other structures such as folds and cleavage. Displacements on the CHT and BHT are highly variable along strike. The CHT has a displacement of 300 m to the north and 2350 m to the south of the ST branch point. The BHT has a displacement of 50 m adjacent to Sub Domain 3c, a displacement of 1000 m (calculated vertical displacement) adjacent to Sub Domain 3b and a displacement of 4800 m adjacent to Sub Domain 3a. These features are discuss in chapter 7.

Shortening values calculated from the cross sections suggest a 49% and 41% total shortening and equivalent thickening for AA' and BB', respectively. Individual shortening calculations for each thrust sheet show a marked general decrease to the NW and coincide with the observed decreasing strain state of surface rocks.

Figure 4.1. Balanced Cross-Sections and Reconstructions: Myponga Thrust System

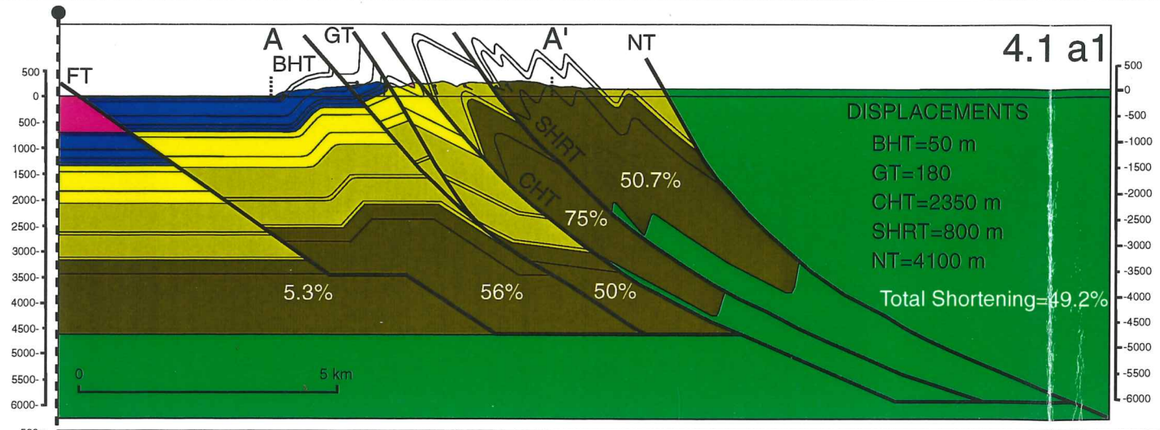

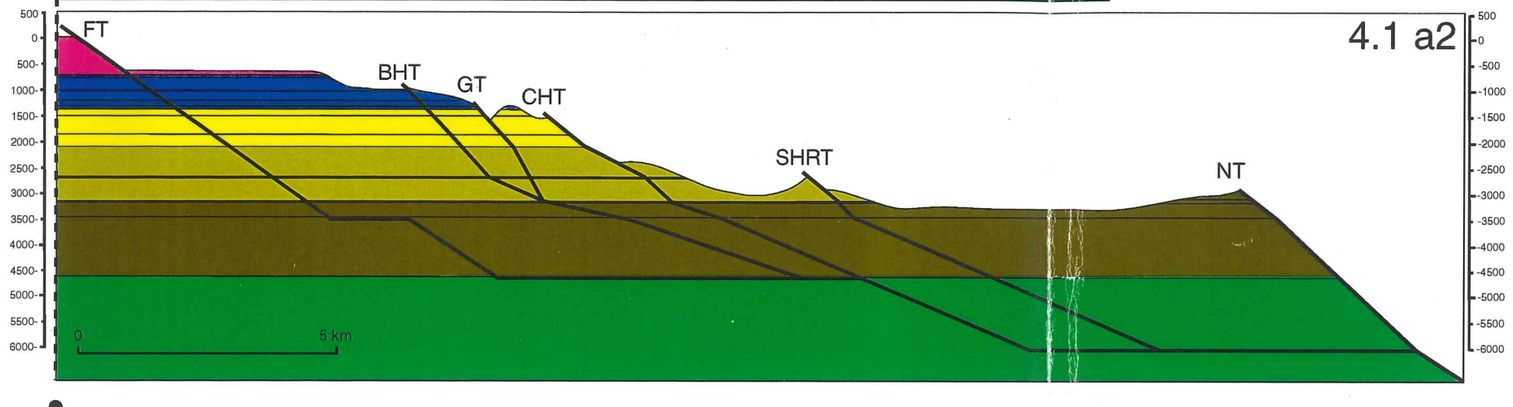

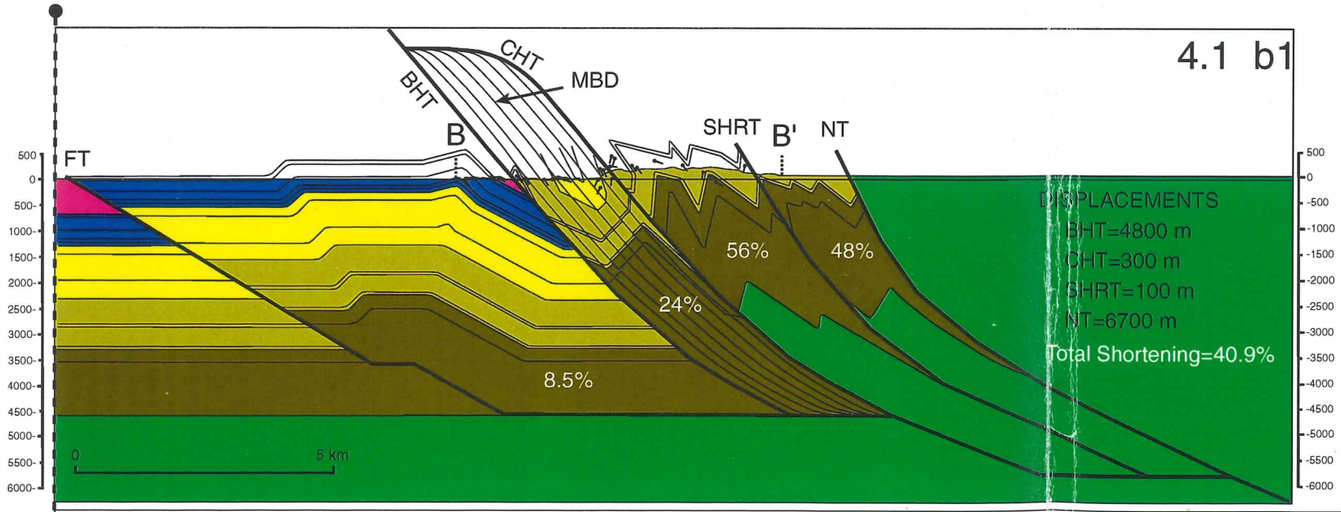

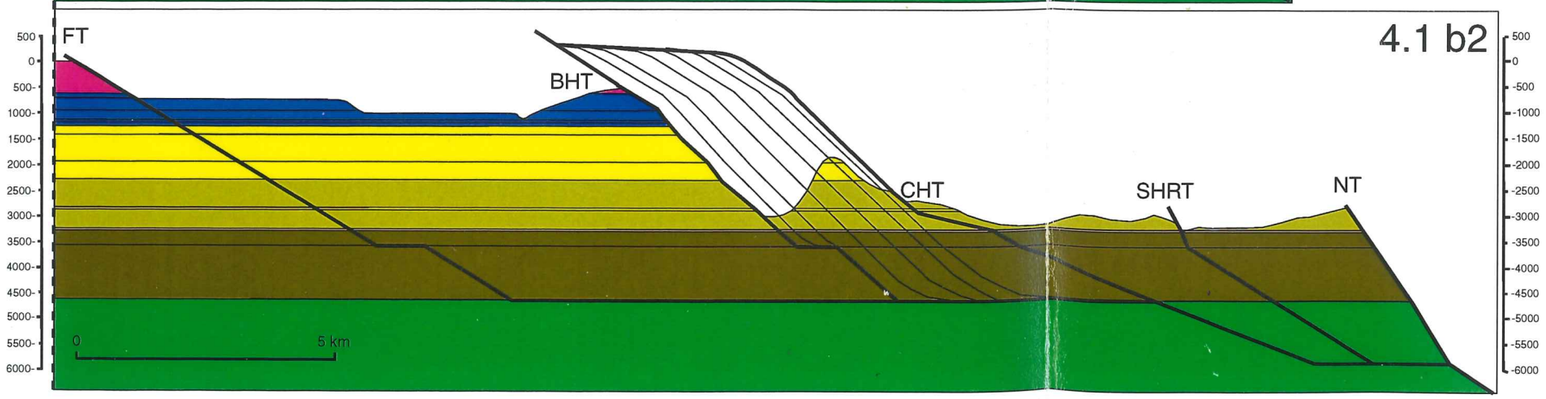

NT	=	Normanville Thrust
SHRT	=	Smith's Hill Road Thrust
CHT	=	Carrickalinga Hill Thrust
MBD	=	Myponga Beach Duplex
GT	=	Goldsmith Thrust
BHT	=	Black Hill Thrust
FT	=	Frontal Thrust (infered and offshore)

- Kanmantoo Group
- Normanville Group
- Wilpena Group
- Umberatana Group
- Burra Group
- Basement

Chapter 5

MICROSTRUCTURE AND KINEMATIC INDICATORS

5.1 INTRODUCTION

In attempting to observe microstructure, determine shear sense and, where possible, the amount of shear it is important to have an oriented sample. The X,Y and Z axes respectively represent the major, intermediate and minor axes of the finite strain ellipsoid (Figure 5.1) Thin sections were cut perpendicular to the foliation (XY) and either parallel (XZ) or perpendicular (YZ) to the X direction of the finite strain ellipsoid. The X direction is generally defined by a stretching lineation within the rock. An oblique cut to the principal strain axes decreases the amount of valuable information obtainable from thin sections and gives an erroneous assessment of the amount of shear and may potentially give a false impression of shear sense.

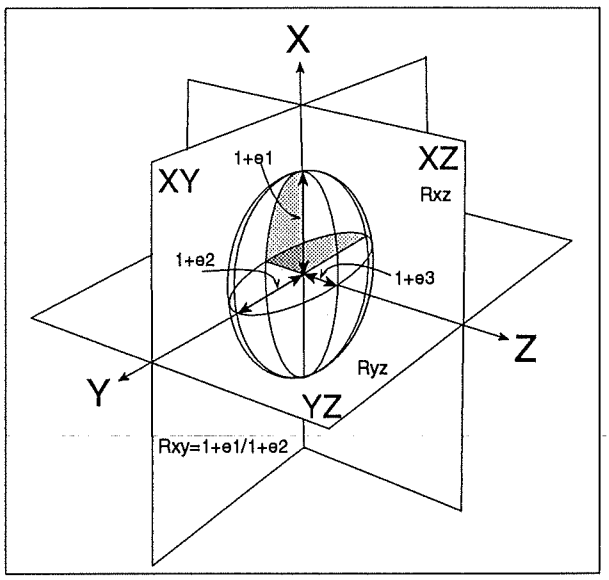

Figure 5.1. The finite strain ellipsoid. Notation for principal strains (e1, e2, e3), principal strain directions (X, Y, and Z), and the principal planes XY, YZ, XZ. RXY, RYZ and RXZ are the principal strain ratios.

5.2 FOLIATIONS

Cleavage foliations are defined by the preferred orientation of inequant mineral grains with long dimensions parallel to cleavage. Within the study area cleavage surfaces were discrete, spaced (.25 mm to 3 mm), anastomosing to parallel zones which were found to be depleted in quartz and rich in opaque and elongate micacous minerals (Plates 3a to c). Approaching major thrusts, cleavage are increasingly prominent. In these zones biotites were found to have increased length/width ratios and grain populations that were more uniformly oriented parallel to cleavage. Both of these features are associated with increasing strain. An uncommon continuous cleavage was observed in siliceous Brighton Limestone and is defined in the XZ section by the maximum elongation direction of quartz and calcite grains and overgrowths (Plates 4f and g). For a more detailed description of cleavage refer to plate 4 descriptions.

5.3 CRENULATION CLEAVAGES

A crenulation cleavage is the microfolding of an earlier foliation, generally defined by the preferred orientation of layer silicates (Hobbs *et al* ., 1976). Locally developed crenulation cleavage (S2) was observed in two samples of Tapley Hill Formation from Domain 2. Plate 3d shows a weathered and incohesive, foliated, fault gouge breccia consisting of loosely bound, angular, yellow sandy fragments with an alignment and preferred augen shape oriented parallel to a cleavage foliation. A suite of rocks exhibiting this fabric defined a zone of shear in the NE of Domain 2 (Map1). The darker phyllitic gouge matrix has a well developed, closely spaced and banded, anastomosing foliation which is deflected by the more competent clasts. Magnification of the pelitic matrix (Plate 3e) shows that the cleavage foliation is crenulated and a discrete, spaced, discontinuous, S2 (vertical) is developed. This cleavage is defined by surfaces enriched in micas that have been rotated toward parallelism with the new foliation and residues of insoluble and opaque material. These generally coincide with the steep limbs of the asymmetric crenulations. Normal dip-slip offsets of the cleavage along the S2 surfaces were prominent. The S2 surfaces are observed to terminate against the more competent clasts and, where there is a competency contrast between foliation bands, the S2 surfaces become discontinuous and arranged in an en echelon fashion. Plate 3e shows the the crenulation cleavage surfaces and crenulations are strongly developed in the mica rich layers but do not penetrate the quartz rich psammitic layers and suggests a strong lithological control upon secondary foliation formation. Plates 3f and g show another example of crenulation cleavage. Bedding, and a weak, near bedding parallel cleavage have been crenulated at a microscale by a second tectonic fabric. The narrowly spaced (1-2 mm), discrete and anastomosing to parallel secondary cleavage surfaces are highlighted by a dark enrichment of aligned phyllosilicates and opaques with quartz being minor or absent. The S2 foliation has an axial planar orientation to a larger scale antiform (Plate 3f) and it is observed to converge or fan from hinge to limb. This fold can therefore be interpreted as a structure formed subsequently to the formation of the first

cleavage by a second phase of deformation which also produced the crenulation cleavage. In the limb of the anticline, bedding laminae are seen to terminate and become step-like in a normal dip-slip manner along secondary cleavage surfaces. A magnification of the hinge zone (Plate 3g) reveals limbs of crenulated bedding which are thinned or offset along S2 surfaces. Both examples of crenulation cleavage show normal dip-slip offsets of earlier foliations along S2 surfaces. These stepped portions indicate either shearing and micro fault formation parallel to the S2 surfaces or dissolution and pressure solution shortening, with compression perpendicular to the S2 surface. If the S2 surface was at some stage inclined to the maximum principal compressional stress, $\sigma 1$, some reverse micro faulting or shear would be expected along with either a micro fault breccia or evidence for ductile crystal deformation. None of these features were observed. Rather, S2 surfaces were associated with reduction in the quartz content and grain size. The diffusion of quartz requires the presence of a fluid phase and the pressure solution shortening is believed to be the deformation process that created the stepped nature of the foliations. Pressure solution shortening is produced by a maximum compression perpendicular to the S2 surface. To quantify the amount of pressure solution shortening methods and calculations from Borradaile (1982) (Appendix 3) were utilised and suggest a pressure solution shortening of 15.8% in zones of intense cleavage formation.

5.4 KINEMATIC INDICATORS

5.4.1 Strain Shadows as Kinematic Indicators

One of the most useful criteria for determining the sense of shear is strain shadow asymmetry (Simpson and Schmid, 1983). Passchier and Simpson (1986) differentiated two rotated porphyroclast systems, σ type and δ type based on strain shadow geometry (Figure 5.2)

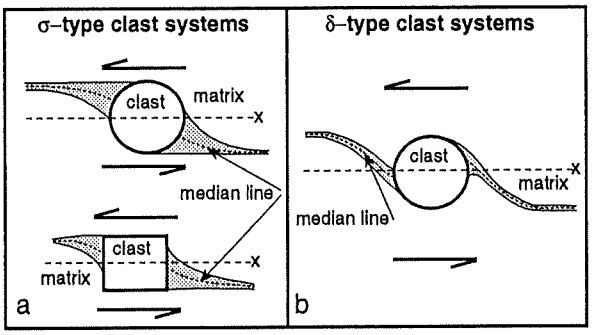

Figure 5.2. Classification of porphyroclast systems showing sinistral sense vorticity, adapted from Passchier and Simpson, 1986. (a) σ Structure - found around porphyroclasts and relates to the form of the dynamically recrystallised pressure shadow tails in relation to the porphyroclasts. In this structure the median line of the tail does not cross the trend of the average schistosity (x) and the structure appears to form because the rotation rate of the tail is higher that of the porphyroclast. This structure is characteristic of shear zones with low shear strains where the recrystalisation rates are higher than the rotation rates. (b) δ Structure - this structure, like the σ structure is developed around porphyroclasts, but where the recrystallised pressure shadow tail is strongly rotated by the porphyroclast. The descriptive name describes the extremely curved and often embayed nature of the generally narrow tail, and where the median line crosses the general trend of the schistosity. This type of structure is particularly characteristic of regions of high shear strain where the recrystalisation rates are lower than the rotation rates.

Sturt Tillite Clast Strain Shadows

Two separate specimens of Sturt Tillite sampled from the hanging wall of the SHRT on each of its study area extremities show high strain shear zone fabrics (Plates 4a and 4b). A fine, dark, horizontal, layer silicate rich cleavage foliation, anastomoses around the more competent and poorly sorted igneous clasts. A preferred orientation of elongate clasts defines an X lineation. Matrix adjacent to clastic boundaries which are normal to the foliation show poor fabric development and are regions related to the deflection of strain around the clasts, termed strain shadows. They are best developed where a high ductility contrast occurs between clasts and a fine grained matrix. Strain shadows are finer and more elongate in plate 4b than in Plate 4a which is indicative of a higher strain history. Simpson and Schmid (1983) suggest that it is generally possible to ascertain the sense of rotation of the clast and hence the shear sense in such rocks by analysis of the asymmetry of strain shadows. Numerous clasts in both Sturt Tillite samples show evidence of rotation and suggest a reverse SE over NW displacement.

Euhedral Pyrite Grain Pressure Shadows

A sample of fine psammitic sandstone from the NW region of Sub Domain 3a contained large euhedral pyrite crystals. Thin sections revealed that the pyrite grains had asymmetric, dynamically recrystallised quartz pressure shadow tails sub parallel to a weak matrix foliation (Plate 3h, figure 5.3). Two crystal growth patterns can be identified in each tail representing two increments of strain. Adjacent to and on opposing sides of the pyrite crystal are large quartz crystals with sigmoidal dynamic growth traces, and adjoining these are beard like clusters of sub parallel quartz fibres. Using figure 5.2 as a comparison, a shear direction can be deduced for the majority of strain shadow systems observed in thin section. These indicate a reverse SE over NW movement.

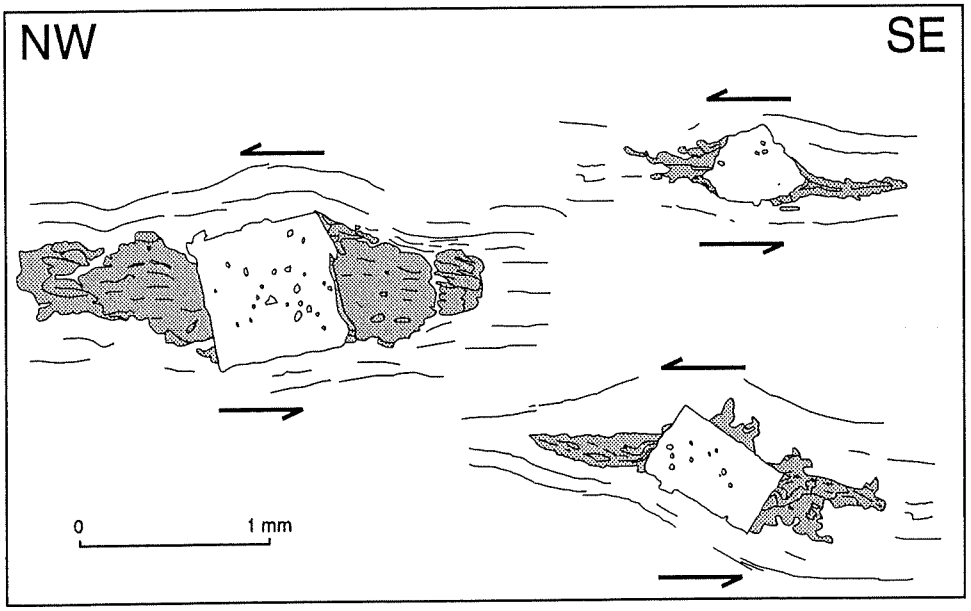

Figure 5.3. Sketches of dynamically crystallised strain shadows around rotated euhedral, pre tectonic pyrite. Asymmetry suggests sinistral movement and in relation to the oriented sample, reverse SE over NW movement.

5.4.2 Brittle-Ductile Veining as a Kinematic Indicator

Numerous extension fissures (tension gashes) were observed in the study area. Tension gashes form in discrete zones of shear which are planar or curviplanar zones of high deformation, are long relative to width and are surrounded by rocks showing a lower state of finite strain. Shear sense may be determined from the orientation of obliquity of the veins with shear zone boundaries. Tension gashes have their tips oriented parallel with the direction of maximum compression, σ1, and are generally infilled with fibrous minerals that grow incrementally in the direction of maximum extension, σ3 (McClay, 1987) (Figure 5.4.a).

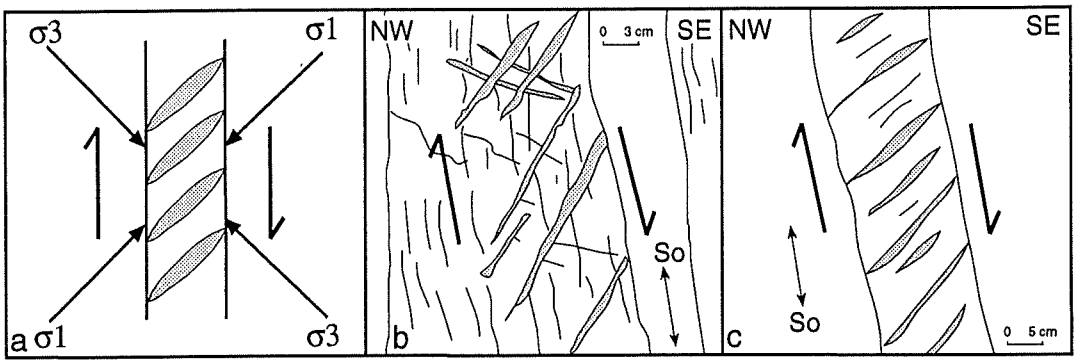

Figure 5.4 Brittle extension veins in shear zones. (a) The tension gashes have their tips oriented parallel with σ1, the direction of maximum compressive stress, and form at 45 to the shear zone boundaries. They are generally infilled with fibrous minerals that grow incrementally parallel to σ3, the direction of maximum extension. (b) A field sketch of conjugate tension gashes from the forward region of sub-Domain 3c. The conjugate nature may be due to a bimodal opposing strain history or principal Reidel and submissive anti-Reidel shears. The dominant veins suggest a normal, SE down movement. (c) A field sketch of tension gashes within sub-Domain 3c. The normal SE down suggested movement is representative of 80% of the veining features in this sub-domain.

Where competency contrasts occur between lithologies, planar en echelon vein systems, which cut across layering transpire, and are distributed evenly along less competent layers. They are the product of bedding parallel brittle simple shear along competent layer boundaries and flexural flow folding. These vein features occur commonly in coastal outcrops of Sellick Hill Limestone of the NW hangingwall regions of Sub Domain 3a (Figure 5.4.c) and less commonly throughout the field area. Rare conjugate vein sets were observed in Sub Domain 3a. Frequently, one vein set was dominant (Figure 5.4 b) and defined the movement direction.

En echelon sigmoidal vein arrays are brittle-ductile shear features and were observed in the more psammitic units in the study area. The sigmoidal vein trace develops during progressive simple shear when initial planar veins are rotated. An example of a dextral sigmoidal en echelon vein array is seen in figure 5.5 and was one of many sets associated with 10 metre folds in the Willochra Subgroup. The majority of vein arrays in Sub Domain 3a indicate normal, SE down kinematics while veins in other domains are indicative of SE over NW reverse movement .

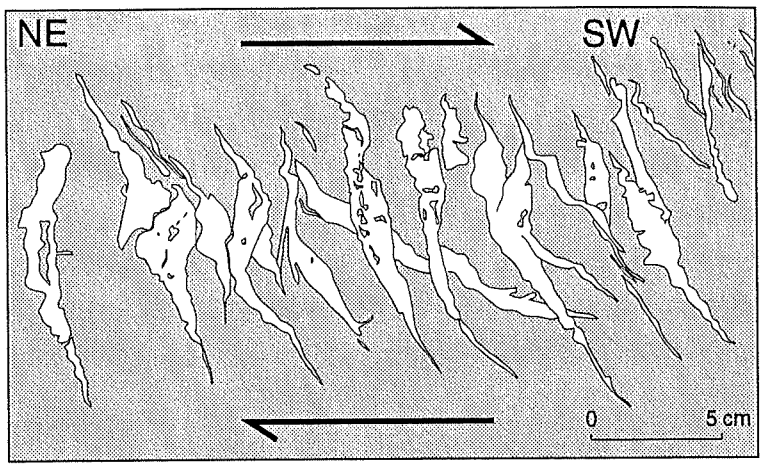

Figure 5.5. A field sketch of sigmoidal enechelon tension gashes in a dextral shear zone in quartzite of the Willochra Subgroup. Indicating oblique movement. This particular vein system was a part of an array of shear zones associated with 15m folds.

Vein fibre orientations, measured from widely spaced localities, were averaged and suggest a maximum extension direction trending 168° and plunging 52° SE and concurs with a SE over NW movement direction.

PLATE 3 DESCRIPTIONS

Plate 3a. This plate shows bedding and cleavage relationships from a sample of Tapley Hill Formation. The inclined, spaced, discontinuous cleavage surfaces are defined by cleavage parallel aligned micas, and a higher content of opaques, which overprint the horizontal compositional bedding laminae. Location 37-4-32. Field of view is 2 mm.

Plate 3b. A moderately spaced and discrete, anastomosing horizontal cleavage in a sample of the SHL. The majority of the rock consists of calcite crystals embedded in a fine calcitic groundmass (75-20%). The discrete cleavage is defined by zones of aligned elongate smaller grains of calcite with a surrounding anastomosing film of dark brown biotite. Location 155-4-1.

Plate 3c. shows a sub-vertical discretely spaced anastomosing to parallel cleavage in fine sandy limestone. The cleavage traces/surface are depleted in quartz and rich in micaceous and opaque minerals. The calcareous laminae are crenulated and their limbs are parallel to cleavage. Cleavage is defined by discrete zones containing elongated and aligned calcite crystals which are smaller than main rock body and a fine elongated biotite fabric which anastomoses around the calcite grains. Location 155-1-6.

Plate 3d. An incohesive fault gauge breccia. Note the preferred orientation of augen shaped psammitic clasts. Location 157-2-17.

Plate 3e. A magnification of the darker phyllitic foliated matrix of plate 3d. Note the vertical crenulation cleavage and its truncation against the lighter more siliceous clasts. Note also the normal dip-slip offsets across S2 surfaces. Field of view, 2 mm.

Plate 3f. Another example of crenulation cleavage (vertical) from the Tapley Hill Formation. Note the dip-slip offsets along S2 surfaces and the relation ship between S2 and the antiform. Location 159-3-3.

Plate 3g. A magnification of the antiformal hinge zone from plate 3f. Field of view is 2mm.

Plate 3h. Quartz pressure shadow tails adjacent to a euhedral pyrite crystal. See text for description. Field of view is 2 mm. Location 37-3-7.

PLATE 3

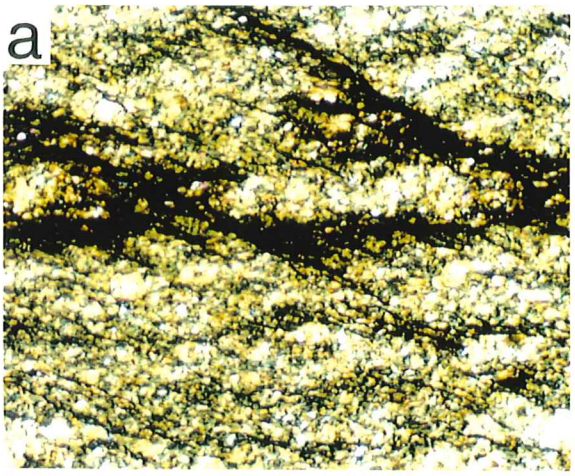

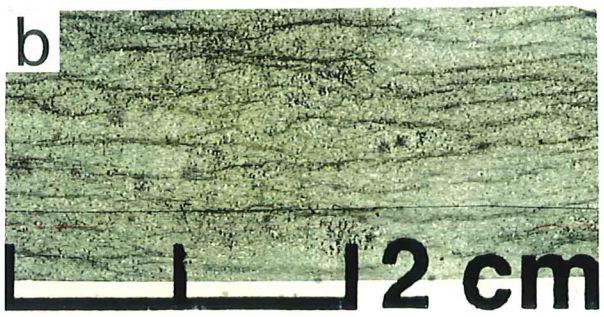

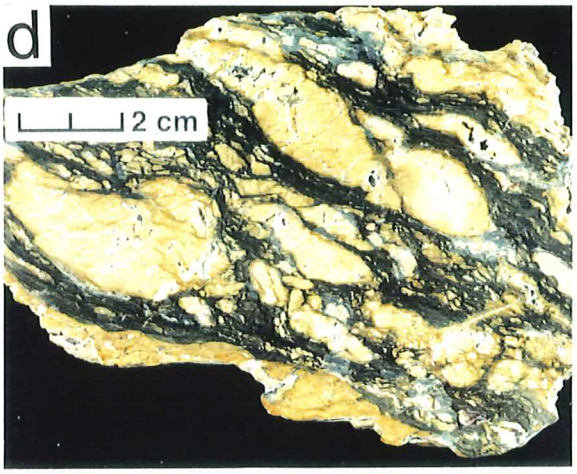

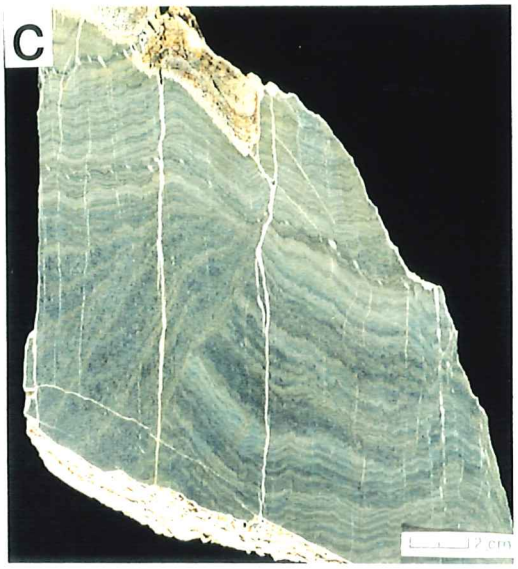

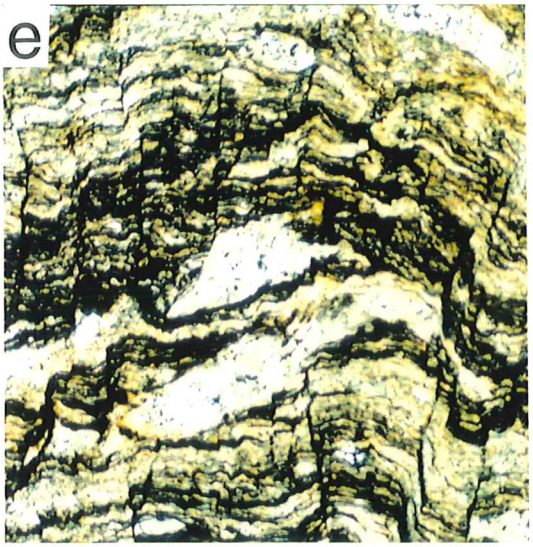

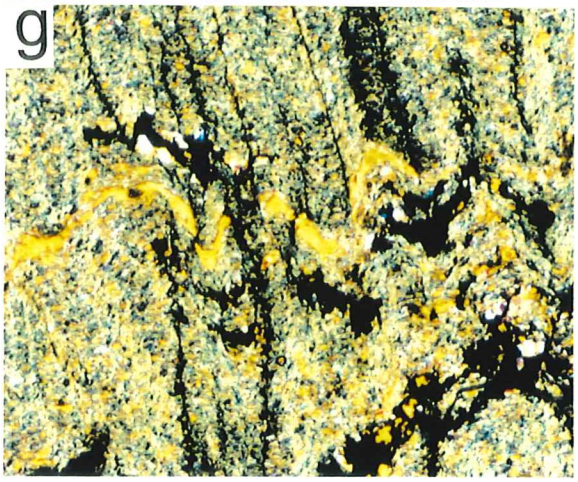

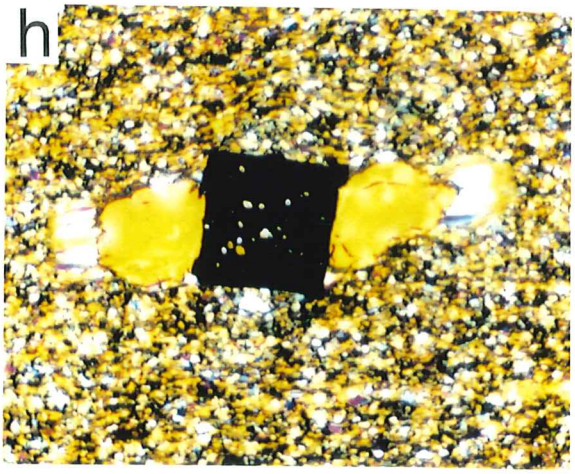

Chapter 6

STRAIN ANALYSIS

6.1 INTRODUCTION

Strain analysis works towards a quantification of geological deformation and involves converting the information on length changes and angular distortions provided by strain markers to a more readily understood representation of the state of strain, generally given by the finite strain ellipsoid (Figure 5.1). Strain is the geometrical expression of the amount of deformation caused by the influence of a system of stresses on a body and is therefore defined as the change in size and shape of a body resulting from the action of an applied stress field (Park, 1989). Strain analysis was undertaken to deduce the three dimensional magnitude and orientations of the local stress field.

6.2 NATURE OF THE STRAIN MARKERS

The Brighton Limestone was found to contain numerous 1-10 cm bands of ferruginous ooids. On the bedding surface they were elongate with the long axis defining an ESE plunging lineation paralleling the thrust transport direction. Oriented samples were taken from the three repetitions of Brighton Limestone in the NW region of Sub Domain 3a (see appendix 1 for precise locations) and XZ and YZ thin sections were made. Under magnification, the two NW most samples (37-3-3a and 6b) could be differentiated from the third (37-3-8) (Plates 4d and e, Plates 4f and g) The two NW samples have larger ooids that contain numerous large singe calcite grains. Sample 37-3-8 was composed of coarse sub-rounded quartz grains and smaller, numerous, highly elongate ooids which are both embedded in a fine calcareous matrix. The ooids are defined by a single dark, fine grained elliptical trace with either a concentric inner facing of fine grained calcite or an undeformed circular calcite crystal. A competency contrast between quartz and large circular calcite grains with the ooids is expressed as a deformation segregation whereby the ooids show the greatest deformation.

6.3 ANALYTICAL PROCEDURES

Enlarged photomicrographs of XY and YZ thin sections provided the raw data of elliptical shapes. These were measured using the numerical software package DIGITIZE (McEachran, 1989). The data sets were transferred and processed by an integrated fabric analysis program INSTRAIN (Erslerv, 1988) to produce graphical Rf/ϕ and Fry strain analysis plots.

6.4 THE FRY METHOD

This technique devised by Fry (1979) is based on the fact that an initially uniform distribution of strain marker centre points will change after deformation into a non uniform distribution. The Fry method was applied to all data sets but showed poor results. This is believed to be a function of the initial ellipse measurement process, where the irregular size and grain spacing was too erratic for adequate results. This method was discarded in favour of the Rf/ϕ method.

6.5 THE Rf/ϕ METHOD

In an aggregate of non spherical sub ellipsoid particles such as oolitic limestone subject to a finite homogenous strain, the final shape and orientation of each particle will depend on five independent variables. These are: (a) the initial shape of the particle, (b) the initial axial orientation, (c) the strain intensity, (d) the strain orientation, (e) the ductility contrast of the particles to the total particle/matrix system (Dunnet, 1969). Ramsay (1967) devised the Rf/ϕ method which allows the effects of initial strain maker shape to be distinguished from those due to tectonic strain. It plots the final deformation axial ratio of an elliptical strain marker (Rf) against the angle between the long axis of a marker and the maximum extension direction in the final or deformed state (ϕ). Using equations from Ramsay, (1983) the undeformed axial ratio of strain marker (Ri) and the strain ratio of the strain ellipse (Rs) were calculated on each XZ and YZ surface from Rf_{max} and Rf_{min} values (ellipticity range) calculated by INSTRAIN.

$$R_i = \left(Rf_{\max} \times Rf_{\min}\right)^{1/2} \qquad \text{(Equation 1.)}$$

$$R_s = \left(Rf_{\max} \times Rf_{\min}\right)^{1/2} \qquad \text{(Equation. 2.)}$$

As a check the values of calculated Rs were again determined by comparing the shape of Rf/ϕ INSTRAIN plots to standard Rf/ϕ curves from Lisle (1985). This reinforced the earlier calculations (see appendix 4 for all Rf/ϕ plots and standard curve comparisons).

6.6 FURTHER ANALYSIS

Using results from the Rf/ϕ method the three dimensional nature of the strain ellipsoid could be calculated. Samples were classified on a Flinn diagram (figure 6.1) which compares and plots the ellipticity of the XY and YZ surfaces. Using equations from Ramsay (1983) the three principal strains e_1, e_2 and e_3, the XY strain ratio and the Flinn diagram parameter k was calculated (refer to Figure 5.1).

$$e_1 = \left(R_s XY^2 / R_s YZ\right)^{1/3} - 1 \qquad \text{(Equation. 3.)}$$

$$e_2 = \left(R_s XY^2 / R_s XY\right)^{1/3} - 1 \qquad \text{(Equation. 4.)}$$

$$e_3 = \left(1 + e_2 / R_s YZ\right) - 1 \qquad \text{(Equation. 5.)}$$

$$RsXY = \left(1 + e_1\right) / \left(1 + e_2\right) \qquad \text{(Equation. 6.)}$$

$$K = \left(R_s XY - 1\right) / \left(R_s YZ - 1\right) \qquad \text{(Equation. 7.)}$$

6.7 RESULTS AND DISCUSSION

The results from INSTRAIN Rf/ϕ and calculations are presented in table 6.1. Strain ratios were found to be higher in the whole rock compared to the internal grains of the ooids and may be a function of competency contrasts and sedimentary compactions, although the highly symmetric nature of the Rf plots suggest no preferred orientation prior to deformation. It is dubious whether the very high strains in sample 37-3-8-b are an accurate representation of the true state of strain in this rock. Strain partitioning due to competency contrasts may exaggerate ooid elongation while the large quartz and calcite grains are unaltered. Ramsay (1983) discusses the difficulties of strain measurements arising from competency contrasts. Samples plotted on a Flinn diagram (Figure 6.1) are classified as oblate and have more or less 'pancake' form. This indicates that the ooids have undergone an apparent flattening, coaxial deformation. The lineation defined by the ooids is parallel to the movement direction. Due to its down dip direction the lineation is believed to be an extensional feature produced by flexural flow folding during the climbing of thrusts or bedding parallel shear. These observations coincide with extensional veining features described in chapter 5.

SAMPLE NUMBER	XZ PLANE	YZ PLANE	Rf max	Rf min	Ri	Rs	e1	e2	e3	Rxy	k
37-3-3-a whole rock	√		21.323	1.250	4.13	5.16	1.17	0.09	-0.58	1.99	0.62
37-3-3-a whole rock		√	6.545	1.016	2.54	2.59					
37-3-3-a ooids	√		11.376	1.213	3.06	3.71	0.82	0.12	-0.66	1.625	0.49
37-3-3-a ooids		√	4.772	1.095	2.09	2.285					
37-3-6-b whole rock	√		20.904	1.050	4.46	4.695	0.90	0.295	-0.595	1.47	0.21
37-3-6-b whole rock		√	8.989	1.136	2.81	3.195					
37-3-6-b ooids	√		6.020	1.007	2.445	2.46	0.405	0.25	-0.43	1.124	0.105
37-3-6-b ooids		√	4.755	1.001	2.180	2.182					
37-3-8-b	√		35.031	3.445	3.19	10.99	2.22	0.06	-0.71	1.23	0.85
37-3-8-b		√	8.175	1.599	2.26	3.62					

Table 6.1. Results of axial ratios from Rf/ϕ plots and subsequent calculations.

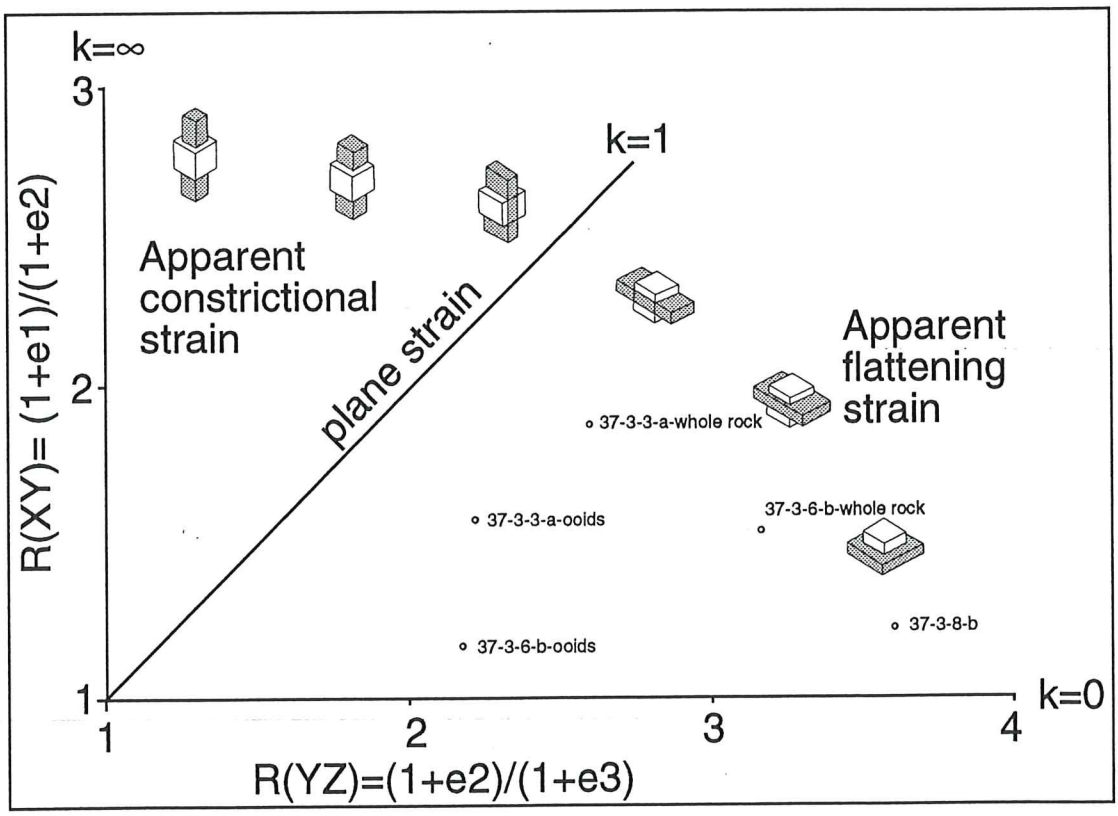

Figure 6.1. The Flinn Graph. A graphical representation of the shape of ellipsoids. All samples plot in the field of apparent flattening and are oblate.

PLATE 4 DESCRIPTIONS

Plate 4a. A sample of strained Sturt Tillite. Note the strain shadows around the large clast, the preferred elongate elongation direction and the fine black foliation (horizontal). Location 159-3-7.

Plate 4b. Another sample of Sturt Tillite. This sample shows a higher state of strain that Plate 4a.

Plate 4c. A photomicrograph of the Sturt tillite showing deflection of the foliation around more competent clasts. The field of view is 2 mm.

Plate 4d. Photograph of Brighton Limestone thin section. Note the large ooids and the internal calcite grains. Elongation defines a horizontal lineation. Location 37-3-6b.

Plate 4e. A Photomicrograph of an ooid. Note the slight elongation in the calcite grains. Field of view is 2 mm.

Plate 4f. Quartz grains in a fine calcite matrix. Ooids are dark elongations and define a continuous cleavage. Note the difference in ooids from plate 4d and e. Note also the lack of elongation in the quartz grains. Field of view is 2cm. Location 37-3-8-b. Field of view is 2 mm.

Plate 4g. At higher magnification the ooids are defined by undeformed circular calcite grains with augen shaped pressure shadows. Field of view is 2 mm.

PLATE 4

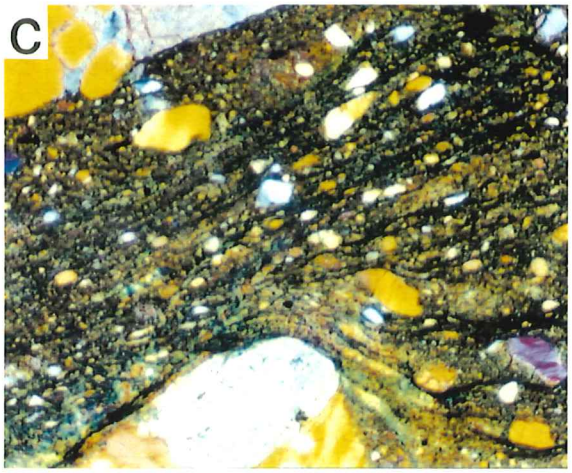

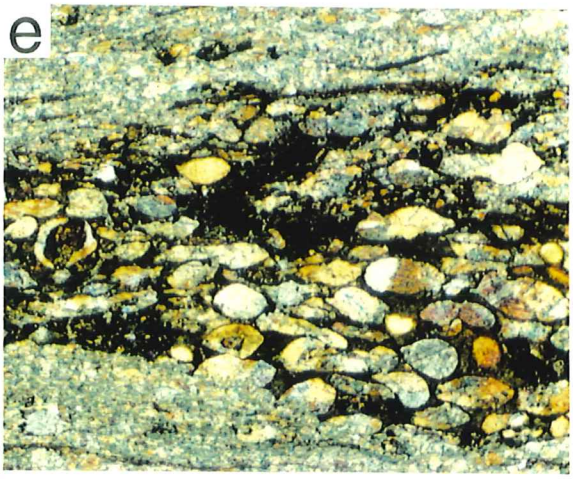

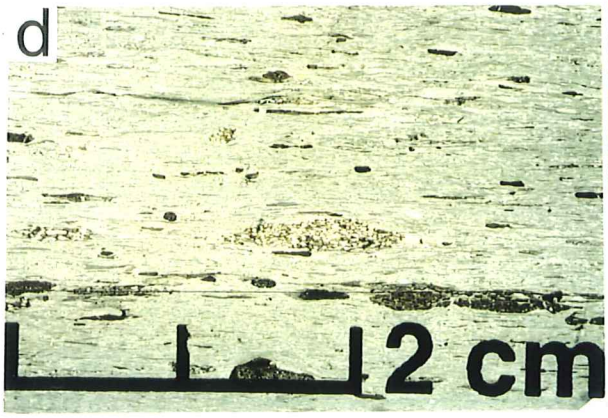

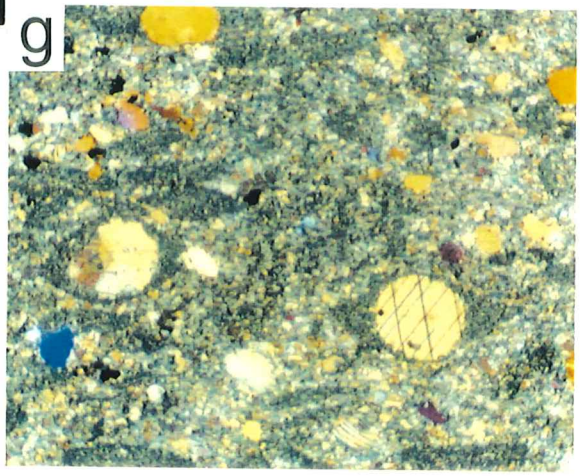

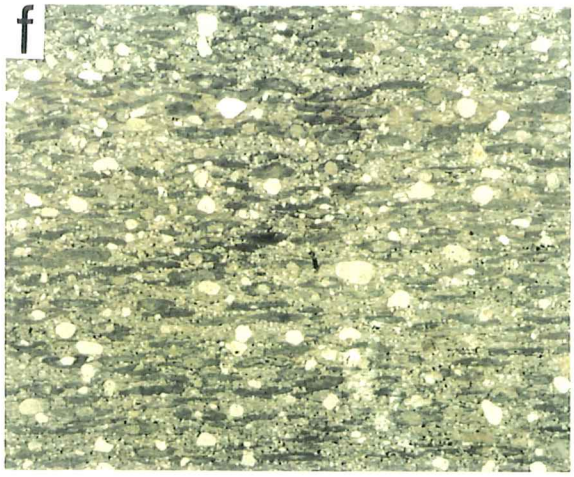

Chapter 7

DISCUSSION

By comparison of figure 7.1 with the cross sections (Figure 4.1) the Myponga Thrust System corresponds to an idealised Coulomb wedge model for the development of a foreland fold and thrust belt (Figure 7.1). Shortening and contraction of the crust by the Delamerian Orogeny can thus be associated with compressional forces acting on the continental lithosphere at plate boundaries or continental collision.

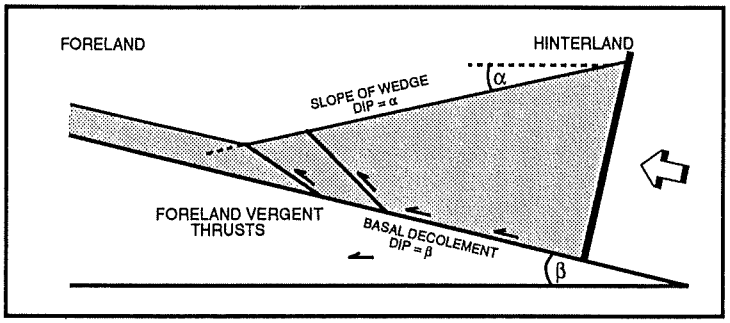

Figure 7.1. Idealised Coulomb wedge model for the development of an accretionary wedge or a foreland fold and thrust belt. Modified from McClay, 1991.

3 DIMENSIONAL GEOMETRY

Within the study area there are numerous structural zones which strike obliquely to the movement direction. This is highlighted by analysis of all minor fold orientations (Figure 7.2a) which shows a complex diversity. Recent studies of foreland fold and thrust belts (Alvarez-Marron, 1995 and Mitra, 1988) suggest that oblique features can result from oblique and lateral ramping within the sole detachment of a thrust sheet (Figure 7.2b). The prominent oblique structural features in the NE of Domain 2 can be explained by oblique ramping at depth.

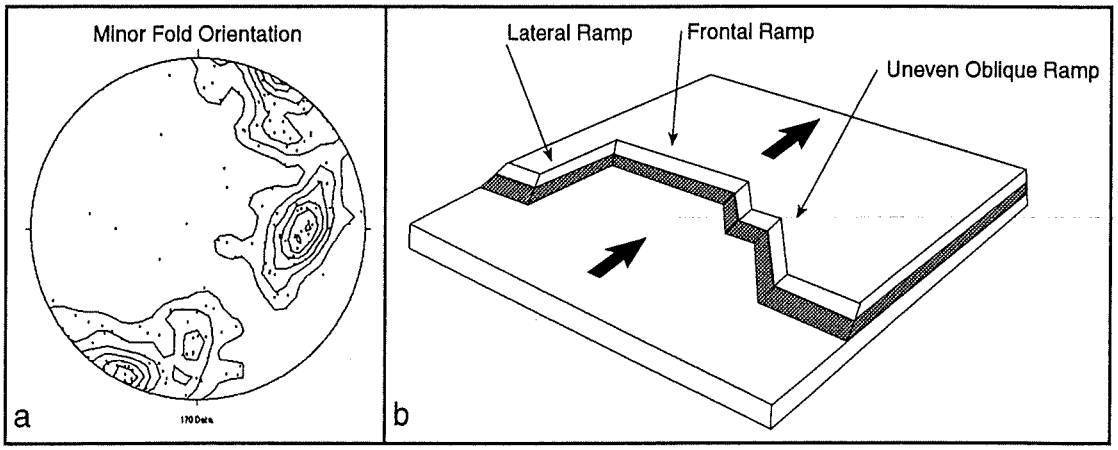

Figure 7.2. (a). Complex monor fold orientations. (b). 3D thrust footwall ramping structures. The uneven nature of the oblique ramp is cognate with those possibly responsible for the complex geometry in the oblique portion of Domain 2. Modified from McClay, 1991.

A rock sample from within the oblique zone of Domain 2 (Plate 3) provided direct field evidence of dextral transpression. This feature would be expected in rocks moving up and across an east-west striking oblique ramp with movement in a northwest direction. A compressional strain component, perpendicular to the strike of bedding surfaces (and the oblique ramp), would form folds with axial traces parallel to the strike of the oblique ramp. At the same time a translational stress component would cause bedding parallel shear in a sub horizontal direction.

The ensuing discussion refers to figure 3.2. Theoretically, corner folds (synclines) should form above the intersection of frontal and oblique ramps. The area labelled 1, in figure 3.2 shows that the kink in the Brighton Limestone coincides with minor folds axes which plunge moderately south, oblique to the transport direction. This area defines a synclinal corner fold axis where a frontal and oblique ramp intersect. The oblique fault (3) and fold axes (4) may be explained by movement over an uneven oblique ramp surface (Figure 7.2b) where complex deformation vectors may cause an intricate pattern of faulting and fold interference. The fault (3) is believed to be discontinuous along strike to the south, where it is presumed to die out into a fold.

Central areas within Domain 2 clearly show oblique structural features (maps 2, 3 and 4). The three dimensional geometric implications of this are unclear and limited outcrop prevented further investigation.

It has been shown in chapter 4 that the CHT and BHT have differential displacements along their trace. This feature can be explained by the evolutionary sequence of thrusting (Figure 7.3a to d).

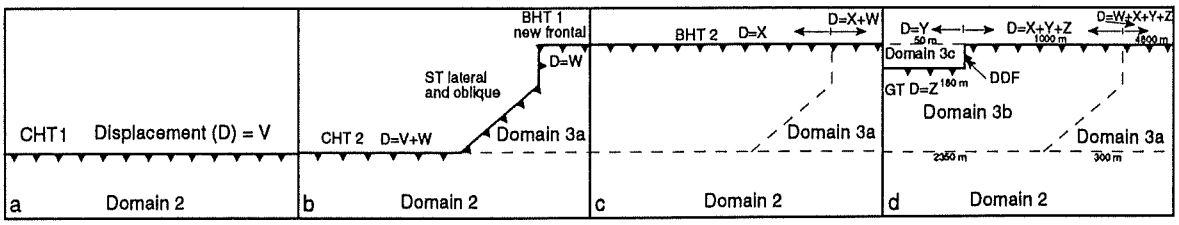

Figure 7.3. Differential displacements along CHT and BHT. An interrelated sequence of thrusting is presented. The theoretical spatial variance in thrust displacement is matched by those calculated from cross sections which validates the thrust interaction sequence.

The scenario presented in figure 7.3 begins at the time when the CHT propagated up through the sedimentary prism (7.3a) and hangingwall displacement is defined as V. Due to increased drag on the fault surface or some other mechanism, displacement along the NE end of the CHT surface ceased and the basal decollement propagated forward (an easier path). Displacement was transferred to another frontal structure BHT 1 (7.3b). An east dipping oblique/lateral connecting splay (the ST) joined CHT 2 and BHT 1, acting as a ramp for hangingwall rocks. The united mass of rock was displaced by an amount, W, and displacement on CHT 2 was V+W (7.3b). The force required to push this rock mass upwards became greater than the force needed to further propagate the basal detachment and slip was once again transferred to another frontal structure, the BHT 2, its position guided by the pre existing weakness of BHT 1. All hanging wall rocks were displaced by X, giving BHT 1 a displacement of W+X (7.3c). Sub domain 3c represents a mass of rock that resisted movement along the BHT and became fused to it shortly after movement commenced (a displacement of Y). The resultant GT and DDF depict an easier propagation path for the continued thrust displacement (displacement of Z), furthermore, they are out of sequence (7.3d). The BHT has theoretical differential displacements of Y, X+Y+Z and W+X+Y+Z adjacent to each subsequent NE sub domain. The true magnitude of fault displacements (7.3d) closely approximates these theoretical equations and therefore suggests that the fault sequence shown in figure 7.3 is accurate. There is a slight disjunction for the displacement adjacent to Sub Domain 3b. A minimum vertical displacement obtained by mapping of 1000 m over, however, where sections were established, displacements of over 2500 m occur. This theoretical method is oversimplified and does not take into account the effects of folding and volume loss processes which are held accountable for this shortcoming.

Sub Domain 3b is fold dominated. The folds in the N are believed to be related to blind thrusts below the surface and thrust displacement is compensated by folding at structurally higher levels (Figure 7.4). The oblique nature of structures west of ST suggest that there is an oblique imbricate thrust system below the surface.

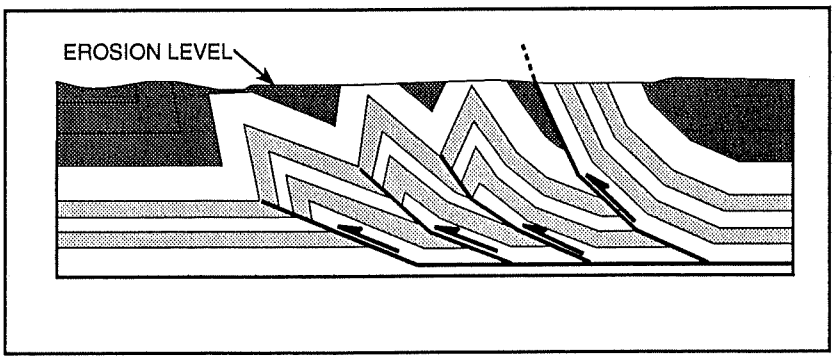

Figure 7.4 Blind thrust system formed in front of an emergent imbricate. Strata overlying the blind thrusts are shortened by folding. This is believed to be the oblique thrust regime below sub-Domain 3b. Modified from McClay, **1991.**

Sub-domain 3a is interpreted as having had a complex deformation history. Propagation of the CHT created a steep to overturned footwall syncline (Figure 7.5a) and concurs with the timing of figure 7.3a. Subsequent contraction forced continued propagation of the basal detachment and the BHT, forming a ramp related hanging wall syncline (Figure 7.5b) and concurs with the timing of figure 7.3b). Further structural thickening developed with the growth of a duplex system which developed as a result of resistance to slip along the basal detachment and resulted in distribution of slip along shallow faults (Figure 7.5c) and concurs with the timing of figure 7.3b,c or d).

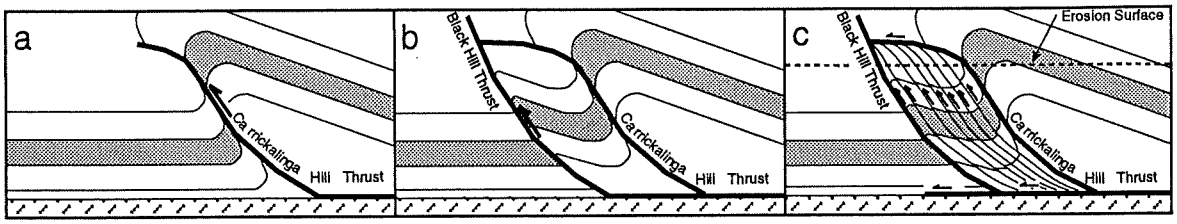

Figure 7.5 Evolution of structures within sub-Domain 3c. (a) Formation of footwall syncline below CHT. (b) Forward most stratigraphy is thrust up along the BHT hanging wall forming the forelimb of a broad syncline. (c) Duplex formation.

Crenulation cleavages and small second phase folds described in chapter 5 are rare and confined to the NE of Domain 2. While it is possible that these structures are related to a second deformational event it is believed that they are the result of a continued deformation associated with oblique ramping.

The majority of kinematic indicators observed in Sub Domain 3a suggest a normal sense movement. Steinhardt (1991) suggests that caution with all sense of shear determinations is necessary because even in a highly non-coaxial deformation opposing senses of shear are often observed and, in fact, should be found. It is possible that deformation with shear in the opposite direction (top to the SE) may have occurred before the Delamerian Orogeny. Preiss (1987) demonstrated that rifting occurred during the early stages of Adelaidean sedimentation in the Proterozoic. Steinhardt (1991) suggested that it is likely that low angle extensional faults were also formed during the Proterozoic in the continental crust underlying the Fleurieu Peninsula and that they would be ideal pre-existing weaknesses on which later compressive stresses of the Delamerian Orogeny can be resolved. There is no further evidence for extensional faulting in the study area and therefore cannot substantiate its occurrence.

COMPARISONS TO THE ANALOGOUS MOINE THRUST ZONE

Studies by Coward and Kim, 1981, and McClay and Coward, 1981 document the structural geometry of the Moine Thrust Zone (MTZ) in the Northwest Scottish Highlands The features are similar to those found in Myponga Thrust System (MTS).

Within the MTZ intensely deformed Proterozoic sediments deformed during the Caledonian Orogeny (500-400 Ma) are thrust NW over a foreland of Palaeoproterozoic Lewisian Gneiss, unmetamorphosed Neoproterozoic and Cambro-Ordovician sediments. There are several thrust sheets stacked on top of each other, the lower most thrust sheet containing an imbricated succession of Cambrian rocks. Displacements on individual thrust vary from 3.5 to 25-30 km. Figure 7.6 shows a cross sections from the MTZ. The outstanding feature is the formation of a duplex zone towards the foreland and its shape and position within the thrust system can be likened to the Myponga Duplex Figure 7.6).

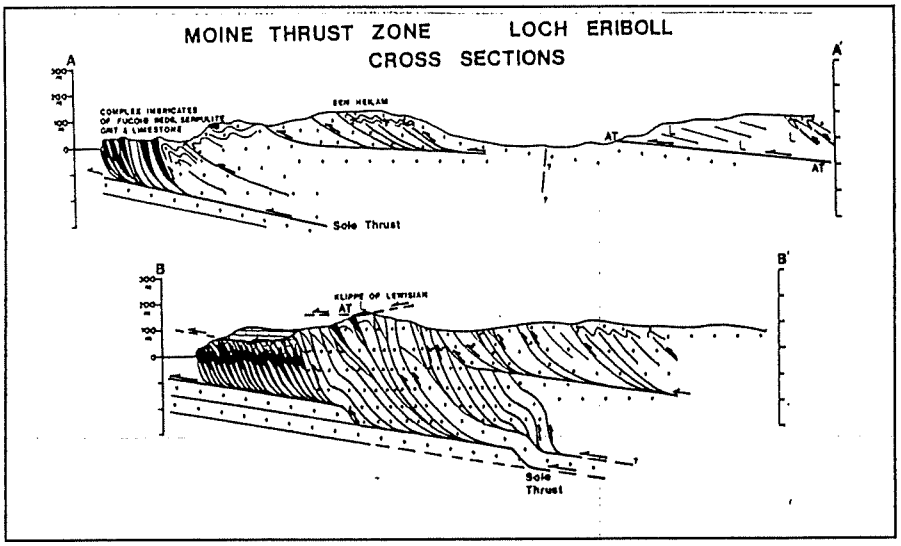

Figure 7.6 Cross sections from the Moine Thrust Zone taken form McClay and Coward, 1981. Note the duplex structures toward the foreland.

Cognate to the MTS the transport direction of the thrusts in the MTZ is to the NW and the sole thrust climbs down the stratigraphy from NW to SE. Thrusts in the MTZ are sharp discontinuities with no deformation above or below. The zone of brecciation on the imbricate faults is less than 1 cm wide and on larger thrusts is only a few tens of centimetres wide, however, many of the hanging wall rocks show evidence of layer parallel shear. Imbricate duplex thrusts in the MTS are discrete and defined by a 5-10 cm zone of intense shear, but generally show high deformation in the hangingwall and less in the footwall. There is evidence of layer parallel shear in the hangingwalls of most major thrusts. In the MTZ oblique imbrication and oblique folds are related to differential movement along a particular thrust plane. This is a definite feature of Domain 3 and the CHT and BHTs. Thrusts in the MTZ are

not always continuous and strain patterns change along strike. These features being controlled by the position of the sole thrust. Structural features vary along strike in Domain 2 of the MTS and are controlled by oblique ramping in the sole thrust. The majority of thrusts in the MTZ are bedding parallel and where the thrusts climb the beds remain parallel to the thrust plane, a feature similar to the MST. Cleavage foliations in the MTZ are defined by grain shape preferred orientations. Pressure shadows are associated with a fluid assisted diffusion (pressure solution) and crenulation cleavages are well developed in more phyllonitic units. These features are all present in the MTS.

The present study shows that the MTS is geometrically similar to the MTZ, although structures are of a smaller amplitude in the latter. The results given here, however show that the deformational processes and geometries are similar in both fold and thrust belts, regardless of the scaling.

CONCLUSION

Detailed geological and structural mapping has exposed a related system of faults associated with the Delamerian contractional event. There are several thrust sheets stacked on top of each other that are linked to a common southeast step-down dêcollement. A shortening of approximately 45% has transpired from major thrusting and folding. Thrust surfaces are generally unseen but are associated with an increase in deformation intensity of hangingwall, and less so, footwall rocks. Individual thrusts have differential displacements along strike. By analysing the spatial variation of displacement, it has been possible to deduce a sequence of thrust emplacement.

Complex minor fold orientations and changes of structural geometry along strike are attributed to oblique and lateral ramp structures in the basal dêcollement surface

Deformation intensity diminishes to the NW and is reflected in the style of structures. A hindward dipping duplex system is developed in one of the more external thrust sheets and is characterised by small, closely spaced imbricate thrusts.

One phase of continued deformation produced a spaced, discrete phylitic cleavage, local crenulation cleavages, strain ratios of up to 11:1 and oblate finite strain ellipsoids.

The structural geometry of the Myponga Thrust System is similar to the Moine Thrust Zone of NW Scotland and is associated with compressional stresses produced by lithospheric plate movements.

ACKNOWLEDGMENTS

Dr Pat James is warmly thanked for his guidance throughout the year. His help was invaluable. Thomas Flottmann is thanked for his assistance with cross section construction and improving the literature. Sherry Proferes was a constant source of help and Geoff, Wayne and Jacie are thanked for their services. I am grateful for the assistance of Jennifer Delurio, Lal Mendis and Ali Yassaghi to improve the literature.
Thanks to MESA for providing the funding for the project.

Special thanks to my fellow structuralists Rebekah, Lyon, Andrew and Dave and to the honours class for their mateship.

Thanks to Jill and Jeff Huxtible for providing excellent accommodation during fieldwork and the Normanville Pub for aiding our cause.

Thanks to my parents for guiding me towards further study and Kelli for her companionship.

REFERENCES

Abele, C., McGowran, B., 1959. The Geology of the Cambrian south of Adelaide (Sellick Hill to Yankalilla). Trans. Roy. Soc. S. Aust., 82: 301-321.

Alvarez-Marron, J., 1995. Three-dimensional geometry and interference of fault-bend folds: examples from the Ponga Unit, Variscan Belt, NW Spain. J. Structural Geol., 17, No. 4: 549-560.

Borradaile, G. J., Bayly, M. B., Powel, C. McA., 1982. Atlas of Deformation and Metamorphic Rock Fabrics. Springer-Verlag, Berlin-Heidelberg.

Campana, B., Wilson, R.B., Whittle, A.W.G., 1955. The Geology of the Jervis and Yankalilla Military Sheets. Rept. Investigations No. 3. Geol. Survey S. Aust.

Clarke, G.L., Powell, R., 1989. Basement-cover interaction in the Adelaide Fold Belt, South Australia: the development of an arcuate foldbelt. Tectonophysics, 158: 209-226.

Coward, M. P., Kim, J. H., 1981. Strain within thrust sheets. In: McClay, K. R., Price, N. J. (Eds), Thrust and Nappe Tectonics. Geol. Soc. London, Spec. Publ., 9: 275-292.

Erslev, E., 1989. INSTRAIN: An integrated analysis program for the Macintosh, Rockware Inc.

Flottmann, T., James, P., Rogers, J., Johnson, T., 1994. Early Palaeozoic foreland thrusting and basin reactivation at the Palaeo-Pacific margin of the southeastern Australian Precambrian Craton: a reappraisal of the structural evolution of the Southern Adelaide Fold-Thrust Belt. Tectonophysics, 234: 95-116.

Fry, N., 1979. Random point distributions and strain measurement in rocks. Tectonophysics, 60: 89-105.

Hobbs, B. E., Means, W. D., Williams, P. F., 1976. An Outline of Structural Geology. John Wiley and Sons, New York.

Hossack, J.R., 1979. The use of balanced cross-sections in the calculation of orogenic contraction: A review. J. geol. Soc. London, 136: 705-711.

Jenkins, R.J.F., 1986. Ralph Tates Enigma - and the regional significance of thrust faulting in the Mt Lofty Ranges. Geol. Soc. Aust., Abs. 15: 101.

Jenkins, R.J.F., 1990. The Adelaide Fold Belt: Tectonic reappraisal. In: Jago, J.B., and Moore, P.S. (Eds), The Evolution of a Late Precambrian-Early Palaeozoic Rift Complex: The Adelaide Geosyncline. Geol. Soc. Aust., Spec. Publ., 16: 396-420.

Lisle, R. J., 1985. Geological Strain Analysis: A Manual for the Rf/ϕ Technique. Pergamon Press, London.

Madigan, C.T., 1925. The Geology of the Fleurieu Peninsula, Part 1: The Coast from Sellick Hill to Victor Harbour. Trans. Roy. Soc. S. Aust., Trans. Proc., 49: 198-212.

Mancktelow, N.S., 1990. The structure of the southern Adelaide Fold Belt, South Australia. In: Jago, J.B., and Moore, P.S. (Eds), The Evolution of a Late Precambrian-Early Palaeozoic Rift Complex: The Adelaide Geosyncline. Geol. Soc. Aust., Spec. Publ., 6: 369-395.

McClay, K.R., 1992. Glossary of thrust tectonic terms. In: McClay, K. R. (Ed), Thrust Tectonics. Chapman ann Hall, London, 419-433.

McClay, K., 1994. The Mapping of Geological Structures. John Wiley and Sons, New York.

McClay, K. R., Coward, M. P., 1981. The Moine Thrust Zone: an overview. In: McClay, K. R., Price, N. J. (Eds), Thrust and Nappe Tectonics. Geol. Soc. London, Spec. Publ., 9: 241-260.

McEachran, D., 1989. DIGITIZE™: Digitising software for the Macintosh. Version 1., Rockware Inc.

Marshak, S., Woodward, N., 1988. Introduction to Cross-Section Balancing. In: Marshak, S., Mitra, G. (Eds), Basic Methods of Structural Geology. Prentice Hall, 303-332.

Mitra, S., 1986. Duplex Structures and Imbricate Thrust Systems: Geometry, Structural Position and Hydrocarbon Potential. Am. Assoc. Pet. Geol. Bull., 70, No. 9: 1087-1112.

Mitra, S., 1988. Three-dimensional geometry and kinematic evolution of the Pine Mountains thrust system, southern Appalachians. Geol. Soc. Am. Bull., 100:72-95.

Offler, R., Fleming, P.D., 1968. A synthesis of folding and metamorphism in the Mt Lofty Ranges, South Australia. J. geol. Soc. Aust., 15 (2): 245-266.

Park, R. G., 1989. Foundations of Structural Geology. Chapman and Hall, USA.

Passchier, C. W., Simpson, C., 1986. Porphyroclast systems as kinematic indicators. J. Structural Geol., 8: 831-843.

Preiss, W. V. (compiler), 1987. The Adelaide Geosyncline-late Proterozoic stratigraphy, sedimentation, palaeontology and tectonics. Geol. Survey S. Aust., Bull., 53.

Ramsay, J. G., 1967. Folding and Fracturing of Rocks. McGraw-Hill, New York.

Ramsay, J. G., Huber, M. I., 1987. The techniques of modern structural geology: Vol 1: Strain Analysis. Academic Press, London.

Ragan, D. M., 1985. Structural Geology. An introduction to Geometrical Techniques. Wiley and Sons, New York.

Segnit, R.W., 1939. The Precambrian-Cambrian succession. Bull. geol. Survey S. Aust., 18.

Suppe, J., Chou, G. T., Hook, S. C., 1992. Rates of folding and faulting determination from growth strata. In: McClay, K. R. (Ed), Thrust Tectonics. Chapman and Hall, London, 141-154.

Simpson, C., Schmid, S.M., 1983. An evaluation of criteria to deduce the sense of movement in sheared rocks. Geol. Soc. Am. Bull., 94: 1281-1288.

Steinhardt, C., 1991. The microstructural anatomy of a major thrust zone on Fleurieu Peninsula, South Australia. Aust. J. Earth Sci., 38: 139-150.

Szmidel, R., 1995. The Structural Geology of Sellick Hill to Myponga Beach, Fleurieu Peninsula, South Australia. BSci. (Hons.) thesis, University of Adelaide (unpubilished.).

Thomson, B.P., 1969. Palaeozoic Era. In: Parkin, L.W. (Ed), Handbook of South Australian geology. Geol. Surv. S. Aust.: 97-108.

APPENDIX 1

Location of samples, fold classifications and plates.

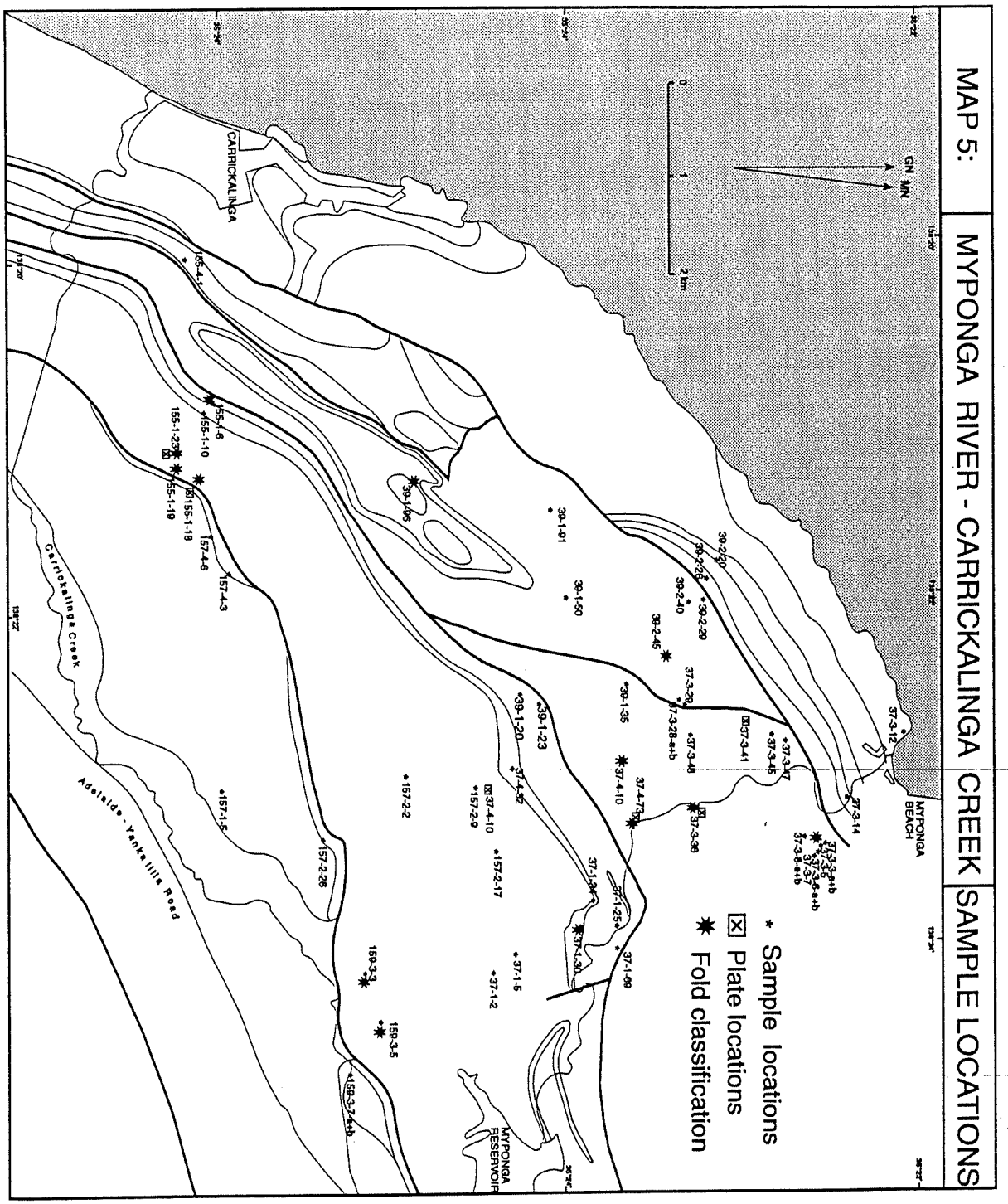

APPENDIX 2

Methods for fold classification

A fold is a distortion of a volume of rock material that manifests itself as a bend or nest of bends in linear or planar elements within the material (Hanson, 1971). Folding occurs when pre existing elements are transformed into new curviplanar or curvilinear configurations, whatever their original condition. Folding almost invariably invokes more than one surface and the geometric relationship between theses adjacent curviplanar surfaces makes up the fold. The geometrical relationship between any two adjacent curved surfaces depends on their relative curvature, and the distance between them. The simplest and most sensitive way of defining this relationship is to construct lines of equal dip, or apparent dip, which are called isogons. The resulting patterns aid in distinguishing accurately between fold forms, but the use of dip isogons also leads to a classification of fold geometry which is simple to apply and easy to remember (Ragan, 1985).

Isogon Construction

(1). Obtain field profiles. Fold profiles were obtained from photos, thin sections and fold profile traces from the field.

(2). Construct a series of dip lines tangent to the curves of two adjacent surfaces. A 10 degree interval was used with exceptions for tight angular folds, where a 20 degree interval was used.

(3). Connect the points of equal dip on the two adjacent curves with a straight line. These are the isogons.

(4). Classify according to table below.

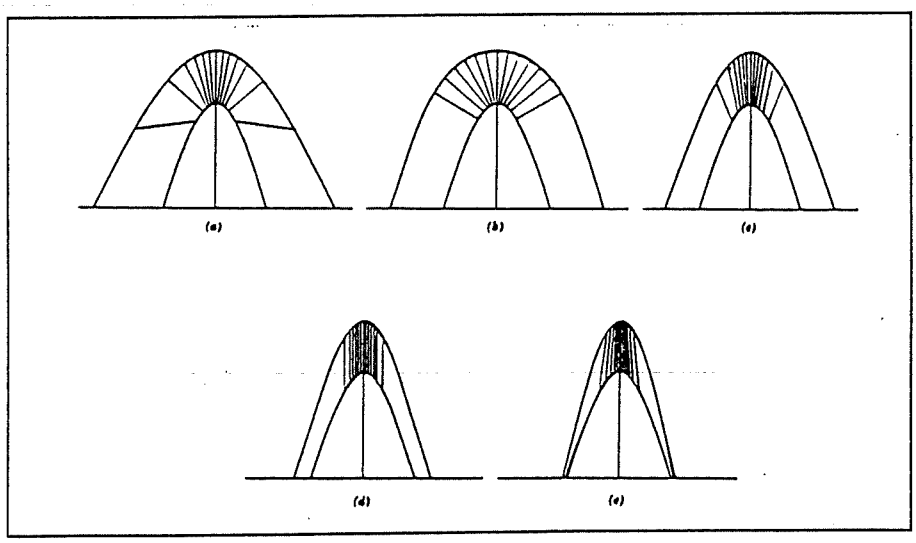

Isogon classification: (a) strongly convergent (1A), (b) parallel (1B), (c) weakly convergent (1C), (d) similar (2), (e) divergent (3) (after Ramsay, 1967).

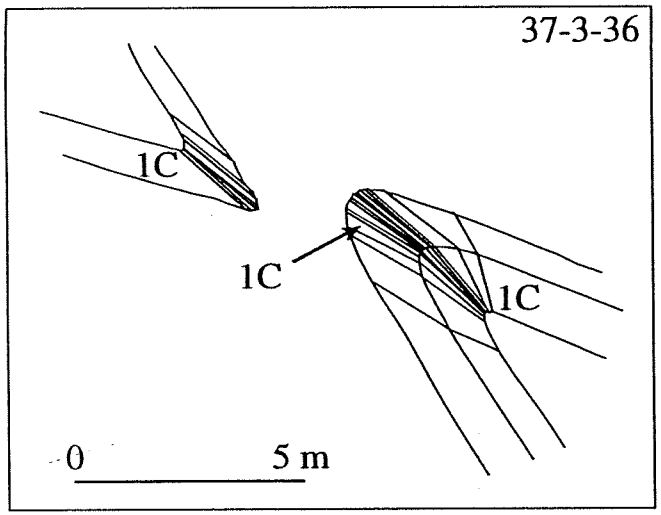

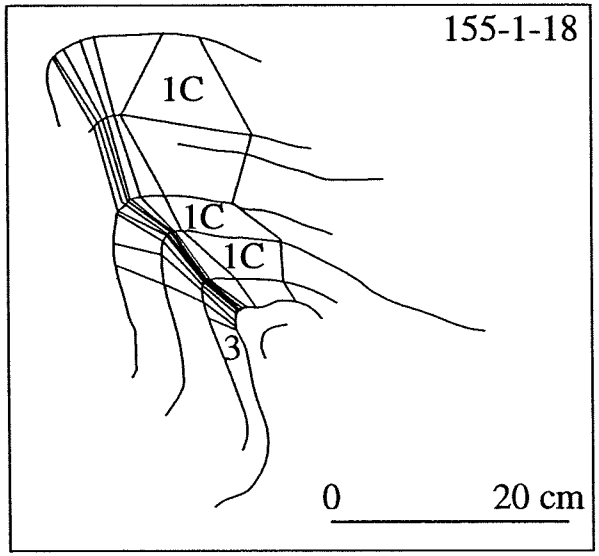

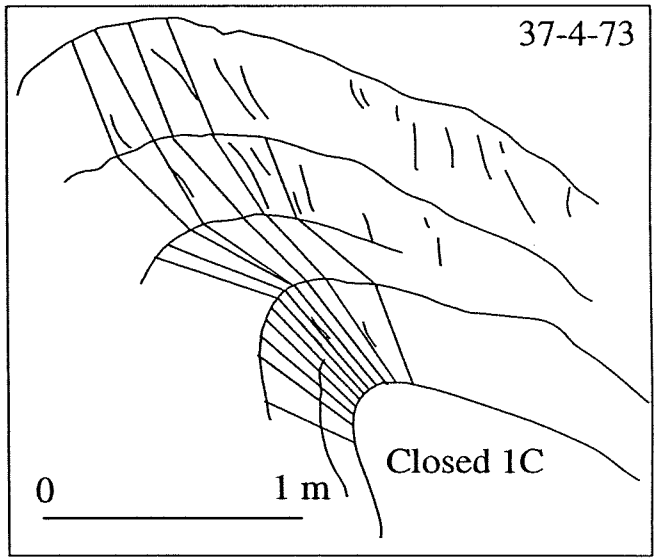

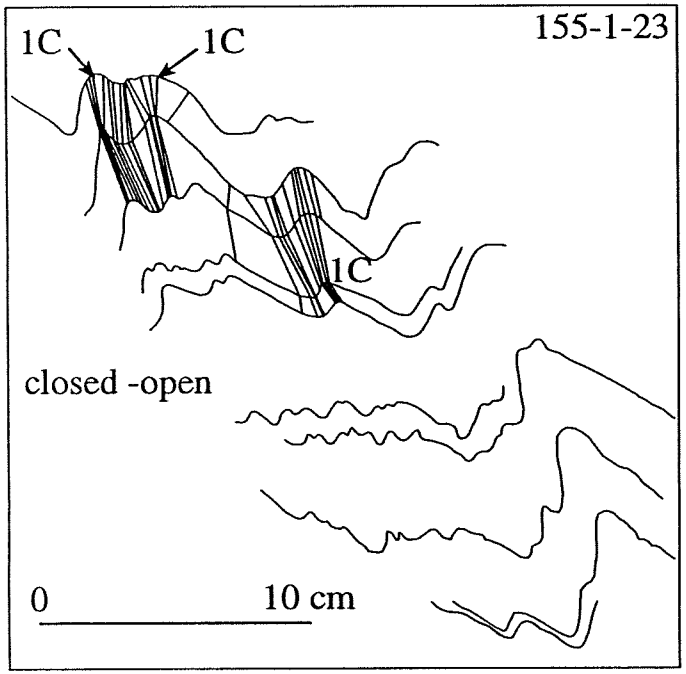

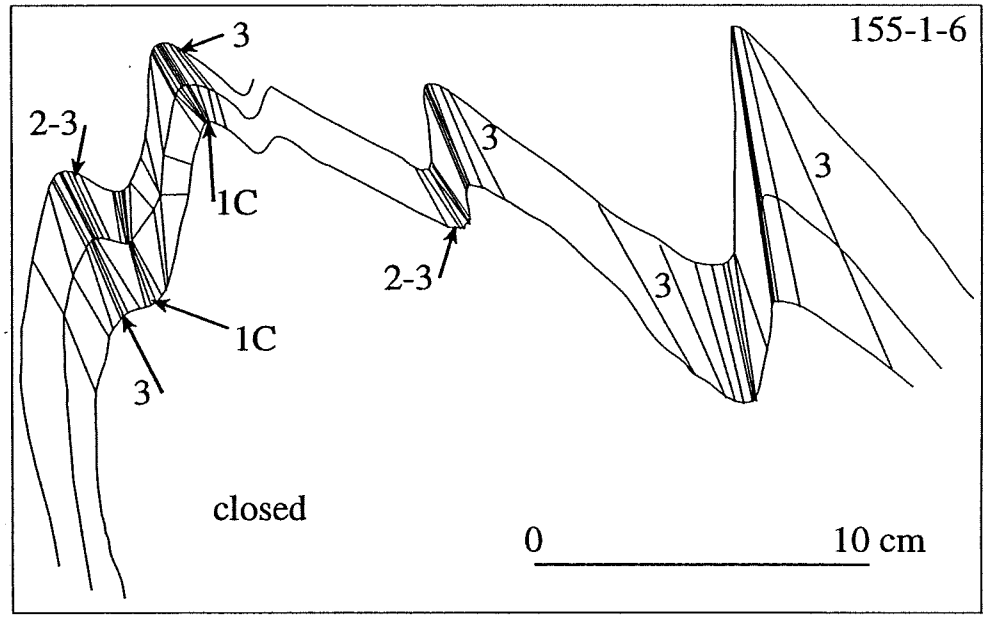

APPENDIX 2 cont.
Examples of fold classification

APPENDIX 3

Quantification of pressure solution shortening

A common feature of rocks with supposed solution cleavage is the production of dip-slip, step-like displacement of earlier foliations or pre cleavage layers (Borradaile, 1982). This is illustrated in (a) and (b) below. If this displacement is due to solution removal it is possible to determine the amount of cleavage removal (χ, in arbitrary units) from the angle between the displaced layers (ϕ) and the displacement (d, in arbitrary units) using the graph.

The average χ for plate 3.f was 0.95 mm

An average of 8.33 cleavage surfaces within 50 mm was calculated suggesting that a shortening of 7.92 mm has occurred within a space of 50 mm.

This represents a 15.8 % pressure solution shortening.

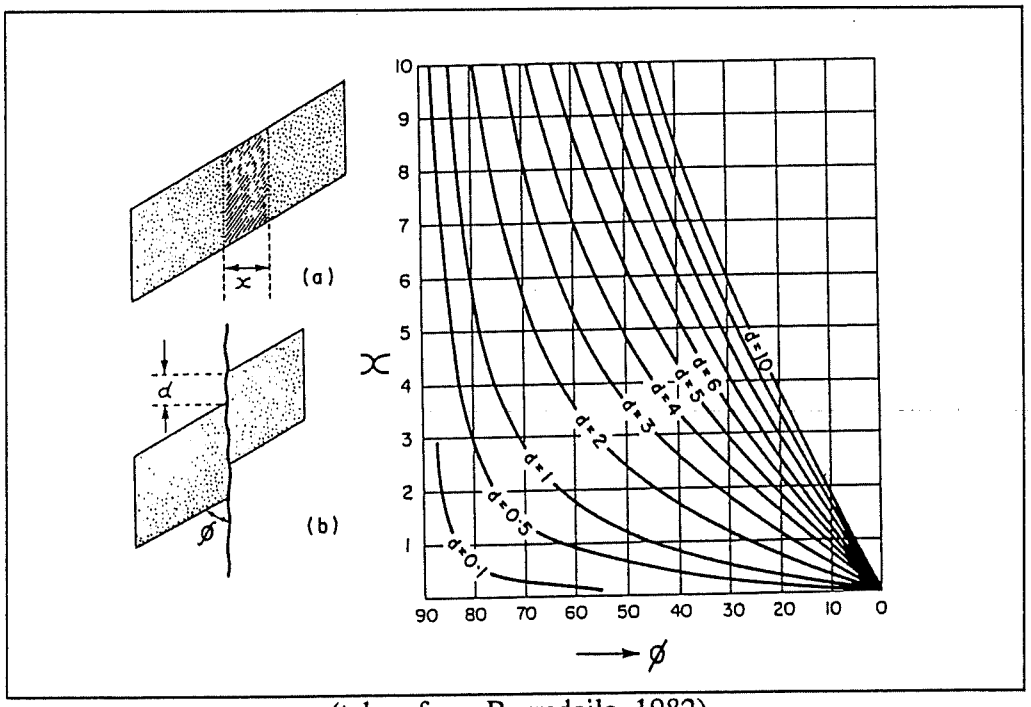

(taken from Borradaile, 1982)

APPENDIX 4

Rfϕ plots and standard Rfϕ comparisons

Project: Strain Analysis: Brighton Limestone
Data File: oolds
Number of Objects: 99 defined by 4 points each.

Sample ID: 37-3-6-b
Surface Orientation: XZ

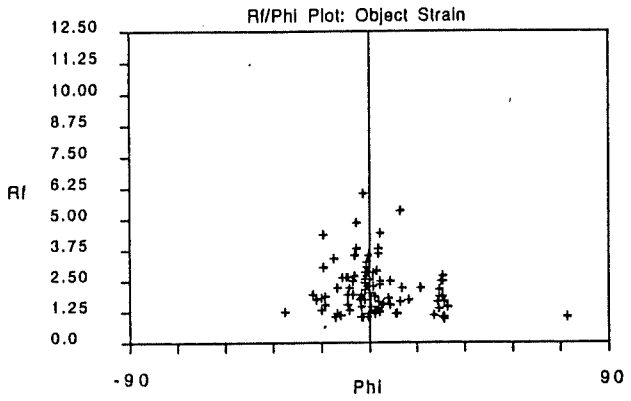

Ellipticity Range: 1.007 to 6.020

MEANS (+/- 1 STD)

Phi (degrees) : 3.044 +/- 15.407
X/Y (n = 99)
Arithmetic 2.128 +/- 0.988
Harmonic 1.787

Mean Object Ellipse: X/Y = 2.040 Phi = -4.14
Average error: 16.03 %

Rs-2.20

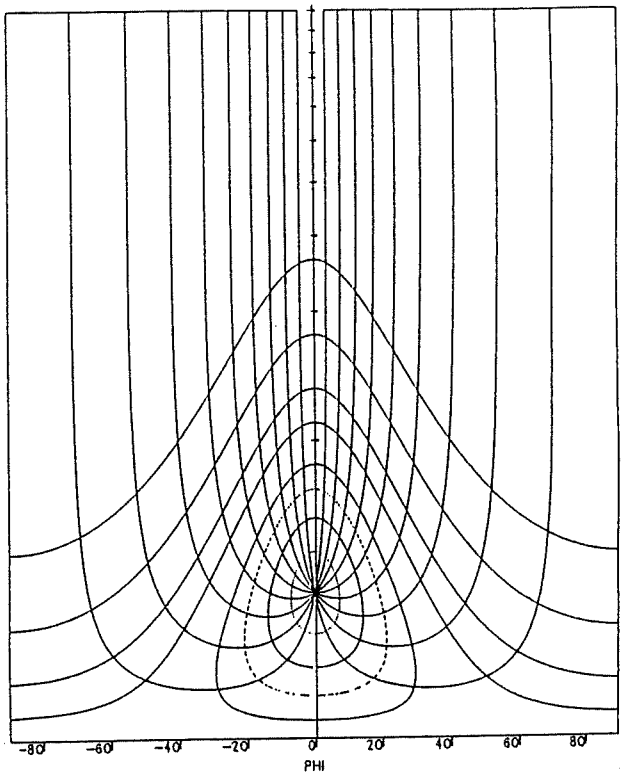

Project: Strain Analysis: Brighton Limestone
Data File: oolds
Number of Objects: 91 defined by 4 points each.

Sample ID: 37-3-6-b
Surface Orientation: YZ

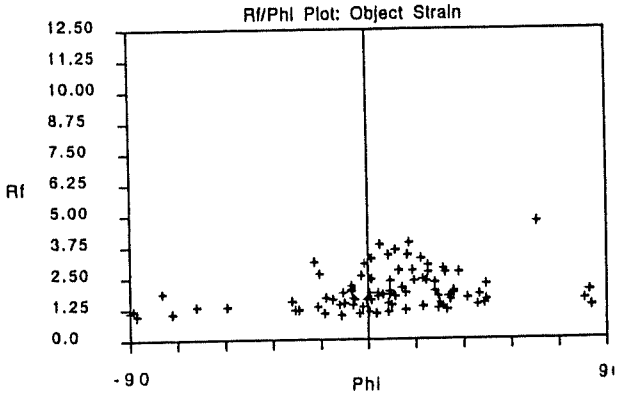

Ellipticity Range: 1.001 to 4.755

MEANS (+/- 1 STD)

Phi (degrees) : 6.031 +/- 32.857
X/Y (n = 91)
Arithmetic 1.936 +/- 0.766
Harmonic 1.701

Mean Object Ellipse: X/Y = 1.624 Phi = 13.38
Average error: 19.03 %

Rs-2.40

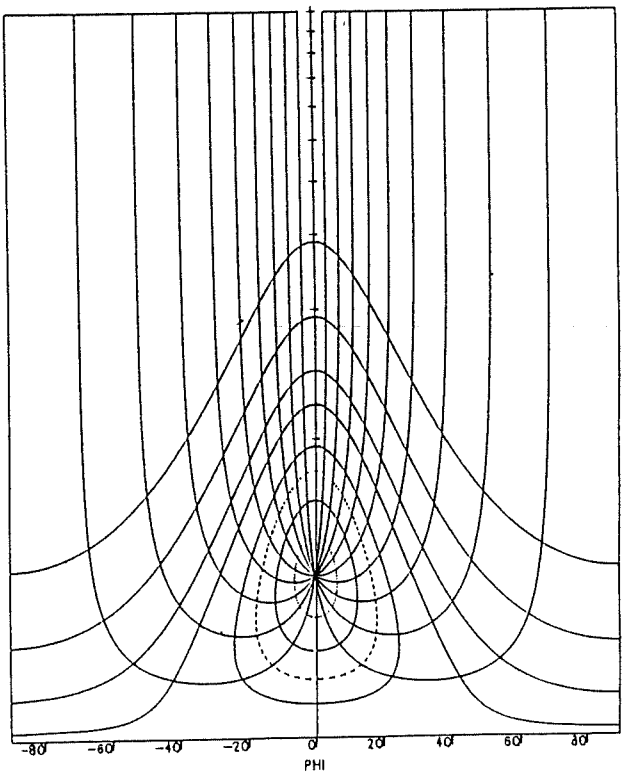

Project: Strain Analysis: Brighton Limestone
Data File: whole rock
Number of Objects: 64 defined by 4 points each.

Sample ID: 37-3-6-b
Surface Orientation: XZ

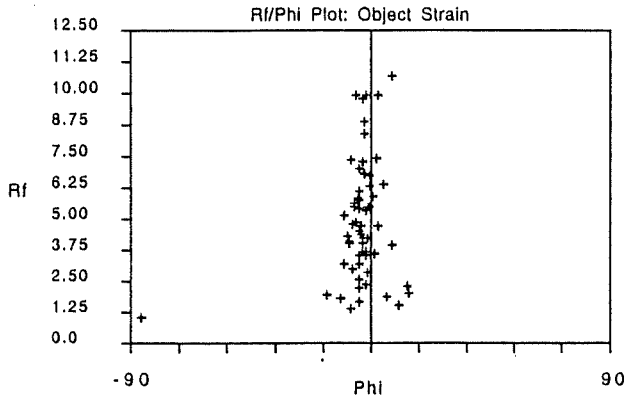

Ellipticity Range: 1.050 to 20.904

MEANS (+/- 1 STD)

Phi (degrees) : -3.877 +/- 11.792
X/Y (n = 64)
Arithmetic 5.403 +/- 3.405
Harmonic 3.823

Mean Object Ellipse: X/Y = 4.560 Phi = -4.14
Average error: 23.92 %

Rs-4.60

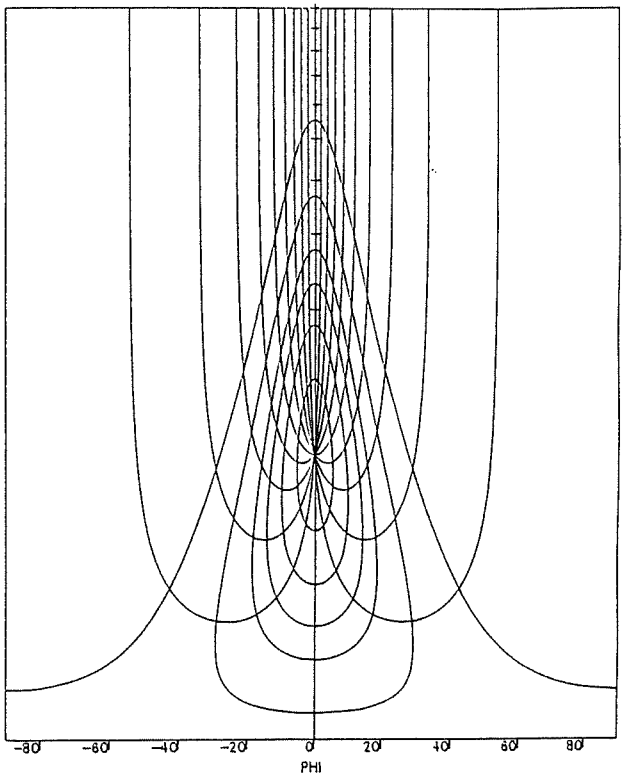

Project: Strain Analysis: Brighton Limestone
Data File: whole rock
Number of Objects: 71 defined by 4 points each.

Sample ID: 37-3-6-b
Surface Orientation: YZ

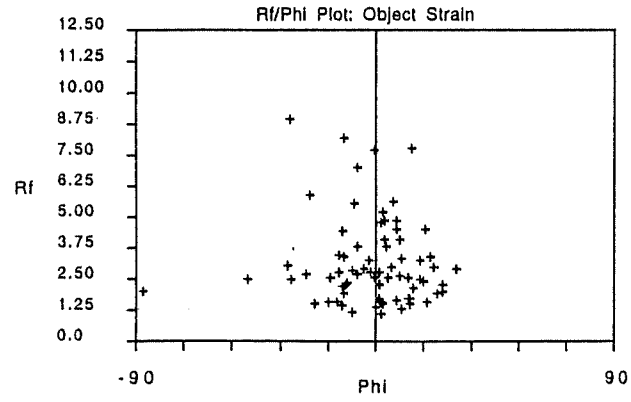

Ellipticity Range: 1.136 to 8.989

MEANS (+/- 1 STD)

Phi (degrees) : -1.816 +/- 18.744
X/Y (n = 71)
Arithmetic 3.183 +/- 1.754
Harmonic 2.511

Mean Object Ellipse: X/Y = 2.883 Phi = -10.95
Average error: 25.04 %

Rs-3.20